

# Electron-deuteron scattering in a current-conserving description of relativistic bound states: formalism and impulse approximation calculations

D. R. Phillips and S. J. Wallace \*

*Department of Physics and Center for Theoretical Physics,  
University of Maryland, College Park, MD, 20742-4111*

N.K. Devine<sup>†</sup>

*General Sciences Corporation, Bowie, MD*  
(October 17, 2018)

## Abstract

The electromagnetic interactions of a relativistic two-body bound state are formulated in three dimensions using an equal-time (ET) formalism. This involves a systematic reduction of four-dimensional dynamics to a three-dimensional form by integrating out the time components of relative momenta. A conserved electromagnetic current is developed for the ET formalism. It is shown that consistent truncations of the electromagnetic current and the  $NN$  interaction kernel may be made, order-by-order in the coupling constants, such that appropriate Ward-Takahashi identities are satisfied. A meson-exchange model of the  $NN$  interaction is used to calculate deuteron vertex functions. Calculations of electromagnetic form factors for elastic scattering of electrons by deuterium are performed using an impulse-approximation current. Negative-energy components of the deuteron's vertex function and retardation effects in the meson-exchange interaction are found to have only minor effects on the deuteron form factors.

## I. INTRODUCTION AND SUMMARY OF RESULTS

Experiments being performed at the Thomas Jefferson National Accelerator Facility (TJNAF) are designed to test our understanding of deuteron properties at space-like momentum transfers comparable to the nucleon mass. In building theoretical models of these processes, relativistic kinematics and dynamics would seem to be called for. Hence, considerable theoretical effort has been invested in constructing relativistic formalisms for the

---

\*Email: phillips@quark.umd.edu, wallace@quark.umd.edu.

<sup>†</sup>Email: devine@quark.umd.edu

two-nucleon bound state that are based on an effective quantum-field-theory Lagrangian. If the usual hadronic degrees of freedom appear in the Lagrangian, then this strategy can be used to obtain a logical extension of the standard non-relativistic treatment of the two-nucleon system. The central goal of such an approach is to capture the relativistic effects in the two-nucleon system. At the same time, for applications to electromagnetic physics, it is critical to embed the Ward-Takahashi identities that imply current conservation for electromagnetic interactions in the theory.

This paper focuses on a three-dimensional (3D) formalism that, in principle, is equivalent to the four-dimensional (4D) Bethe-Salpeter formalism. This approach has been developed in two recent papers [1,2]. We review the formalism for relativistic bound states, and provide an extension that ensures nonsingular behavior of the interaction in frames where the total momentum of the bound system is nonzero. We also construct the corresponding electromagnetic current. Calculations of elastic electron-deuteron scattering are performed based upon the impulse approximation and the results for the observables  $A$ ,  $B$  and  $T_{20}$  are presented.

The Bethe-Salpeter equation,

$$T = K + KG_0T, \quad (1.1)$$

for the four-dimensional  $NN$  amplitude  $T$  provides a theoretical description of the deuteron that includes relativity. In Eq. (1.1),  $K$  is the Bethe-Salpeter kernel, and  $G_0$  is the free two-nucleon propagator. In a strict quantum-field-theory treatment, the kernel  $K$  includes the infinite set of two-particle irreducible  $NN \rightarrow NN$  Feynman graphs. Numerical methods to calculate the 4D t-matrix of Eq. (1.1), with an infinite kernel containing all crossed ladders, have been developed and demonstrated for a simple scalar field theory by Nieuwenhuis and Tjon [3].

For the two-nucleon system, such an application of the full effective quantum field theory of nucleons and mesons is not only impractical, it also is inappropriate because hadronic degrees of freedom are not fundamental. Rather, the Bethe-Salpeter formalism serves as a theoretical framework within which a relativistic effective interaction may be developed. This is entirely analogous to the way that the Schrödinger equation serves as a framework for development of a non-relativistic potential that describes the  $NN$  phase shifts. Since the  $NN$  interaction is an effective one, it is equally appropriate to develop the relativistic effective interaction within an equivalent three-dimensional formalism that is obtained from the four-dimensional Bethe-Salpeter formalism via a systematic reduction technique.

In Ref. [1], a 3D reduction of the Bethe-Salpeter formalism was developed such that the resulting equations involve the same propagator as appears in the Salpeter equation [4],

$$T_1 = K_1 + K_1\langle G_0\rangle T_1. \quad (1.2)$$

The three-dimensional propagator  $\langle G_0\rangle$  is obtained by integrating over the time-component of relative momentum,

$$\langle G_0\rangle = \int \frac{dp_0}{2\pi} G_0(p; P). \quad (1.3)$$

The 3D kernel is defined by solving two coupled equations,

$$K_1 = \langle G_0 \rangle^{-1} \langle G_0 K \mathcal{G} \rangle \langle G_0 \rangle^{-1}, \quad (1.4)$$

which is three-dimensional, and

$$\mathcal{G} = G_0 + G_0(K - K_1)\mathcal{G}, \quad (1.5)$$

which is four dimensional. In fact, the condition (1.4) is obtained by demanding that  $\langle \mathcal{G} \rangle = \langle G_0 \rangle$ . (See Ref. [1] for details. Other works which have considered a similar formalism include Refs. [5–9].) This formalism is systematic in the sense that, given a perturbative expansion for the 4D kernel,  $K$ , a perturbative expansion for the 3D kernel,  $K_1$ , can be developed. However, it is necessary for  $\langle G_0 \rangle$  to be invertible in order for the 3D reduction to contain the full content of the 4D theory.

As mentioned above, when  $G_0$  is the standard two-particle propagator of the Bethe-Salpeter formalism,  $\langle G_0 \rangle$  is the 3D Salpeter propagator. For spin-1/2 particles it is,

$$\langle G_0 \rangle = \frac{\Lambda_1^+ \Lambda_2^+}{P^0 - \epsilon_1 - \epsilon_2} - \frac{\Lambda_1^- \Lambda_2^-}{P^0 + \epsilon_1 + \epsilon_2}; \quad (1.6)$$

where  $\Lambda^\pm$  are related to projection operators onto positive and negative-energy states of the Dirac equation,  $P^0$  is the total energy of the two-body system, and

$$\epsilon_i = (\mathbf{p}_i^2 + m_i^2)^{1/2}. \quad (1.7)$$

Here, and throughout the paper, these single-particle energies are to be understood as having an infinitesimal negative imaginary part. This defines our  $i\epsilon$  prescriptions. Note that for spin-half particles, the equal-time propagator of the Salpeter equation is defined only on two of the four sectors of the Dirac space of two particles. It is not invertible. Although consistent equations can be projected out for the  $++$  and  $--$  components, one must set the  $+-$  and  $-+$  components to zero for consistency. Consequently, the 3D reduction does not have the full content of the 4D theory. If the 4D and 3D theories are to have the same dynamical content then we must include graphs involving  $+-$  states, such as the time-ordered Z-graph of Fig. 1, in both. This graph is not contained in the ladder Bethe-Salpeter equation scattering series.

The absence of this mechanism from the ladder Bethe-Salpeter equation is related to the fact that if we allow one particle's mass to tend to infinity, the propagator does not reduce to the Dirac propagator for the other particle. Consequently, Eq. (1.2) does not possess the correct one-body limit if any finite set of graphs is chosen for  $K_1$ .

If a scattering equation with a kernel which contains only a finite number of graphs is to possess the correct one-body limit, two distinct criteria must be satisfied. First the 3D propagator should limit to the one-body propagator for one particle (either Dirac or Klein-Gordon, depending upon the spin) as the other particle's mass tends to infinity. Second, as either particle's mass tends to infinity, the equation should become equivalent to one in which the interaction,  $K_1$ , is static.

In fact, Eq. (1.2)'s lack of either of these properties springs directly from the Bethe-Salpeter equation (1.1) not having the correct one-body limit if the kernel does not include the infinite set of crossed-ladder graphs. As alluded to above, solution of the Bethe-Salpeter

equation with such a kernel is impractical in the  $NN$  system. Nevertheless, the desired properties may be obtained by using a 4D integral equation for  $K$  to reorganize the contributions to the kernel of the Bethe-Salpeter equation as follows,

$$K = U + UG_C K. \quad (1.8)$$

Given a suitable choice for  $G_C$ , this equation defines a reduced kernel,  $U$ , in terms of the original kernel,  $K$ . The propagator,  $G_C$ , is chosen so as to separate the parts of the kernel,  $K$ , that are necessary to obtain the one-body limits from the parts that are not. Once this is done,  $U$  may be truncated at any desired order without losing the one-body limits. It is readily seen that the original kernel  $K$  may be eliminated in favor of the reduced one,  $U$ , so as to obtain the following 4D equation for the t-matrix, which is equivalent to Eqs. (1.1) and (1.8),

$$T = U + U\mathcal{G}_0 T, \quad (1.9)$$

where

$$\mathcal{G}_0 \equiv G_0 + G_C. \quad (1.10)$$

We are now in a position to remedy the defects of our previous three-dimensional reduction. Applying the same 3D reduction procedure as above to this new 4D equation produces

$$T_1 = U_1 + U_1 \langle \mathcal{G}_0 \rangle T_1, \quad (1.11)$$

where the 3D propagator is

$$\langle \mathcal{G}_0(P) \rangle = \frac{\Lambda_1^+ \Lambda_2^+}{P^0 - \epsilon_1 - \epsilon_2} - \frac{\Lambda_1^+ \Lambda_2^-}{2\kappa_2^0 - P^0 + \epsilon_1 + \epsilon_2} - \frac{\Lambda_1^- \Lambda_2^+}{P^0 - 2\kappa_2^0 + \epsilon_1 + \epsilon_2} - \frac{\Lambda_1^- \Lambda_2^-}{P^0 + \epsilon_1 + \epsilon_2}, \quad (1.12)$$

and  $\kappa_2^0$  is a parameter that arises from the eikonal approximation. This 3D propagator is found by integrating the four-dimensional propagator over the time component of relative momentum. In configuration space this action is equivalent to considering the propagator in which the two particles involved are considered only on equal time slices. Thus this will be referred to as the ET propagator. It was derived for use with instant interactions by Mandelzweig and Wallace [10,11] with the choice  $\kappa_2^0 = P^0/2 - (m_1^2 - m_2^2)/(2P^0)$ . It has the correct one-body limits as either particle's mass tends to infinity and has an invertible form. Meanwhile, the 3D kernel  $U_1$  is systematically defined by two equations that are obtained from Eqs. (1.4) and (1.5) by the substitutions  $K \rightarrow U$ ,  $K_1 \rightarrow U_1$  and  $G_0 \rightarrow \mathcal{G}_0$ .

Equation (1.11) is a 3D scattering equation that incorporates relativistic effects systematically and has the correct one-body limit. Numerical calculations by Nieuwenhuis and Tjon [3], and in our previous paper [1], suggest that the three-dimensional equation with a lowest-order kernel provides a good approximation to the relevant physics of the full scattering series of ladders and crossed ladders.

Negative-energy states and thus Z-graphs, such as the one shown in Fig. 1, are included in the 3D formalism in a way that is symmetrical with respect to interchange of particle labels. When the terms in the propagator involving  $\Lambda_2^-$  are omitted, it takes a form that is very similar to the 3D propagator of the spectator formalism of Gross [12], as derived with

particle 1 on mass shell. Correspondingly, when the terms in the propagator involving  $\Lambda_1^-$  are omitted, the propagator is very similar to that of the spectator formalism, derived with particle 2 on mass shell. Indeed, in  $++$  sectors, Eq. (1.12) is the same as either of these spectator propagators, and thus differences arise only because of the negative-energy states. Usually for the  $NN$  system, a symmetrized form of the spectator propagator is used, and this is obtained by averaging the propagators derived with particle 1 and particle 2 on mass shell [13]. However, because of averaging, the symmetrized spectator propagator has half the propagation amplitudes of the ET propagator in  $+-$  and  $-+$  states. A similar comparison may be made with the BSLT quasipotential propagator of Blankenbecler-Sugar [14] and Logunov-Tavkhelidze [7] that has been used in the work of Hummel and Tjon [15–17]. The BSLT propagator also has half the propagation amplitudes of the ET propagator in  $+-$  and  $-+$  states. Because similar couplings to the  $+-$  and  $-+$  states are present in all of these approaches when similar meson exchange interactions are used, we would expect the role of negative-energy states to be larger when the ET propagator is used than when either the spectator propagator of Gross or the BSLT propagator of Hummel and Tjon is used.

A straightforward analysis of time-ordered perturbation theory graphs for the  $NN$   $t$ -matrix in the static limit (see Appendix A) shows that the leading Z-graphs involving the intermediate  $+-$  and  $-+$  states are correctly given by the ET propagator. Results based upon either the symmetrized Gross propagator or the BSLT propagator are too small by a factor of two.

Our preference for the ET formalism is based on three facts: it embeds the correct one-body limit for *either* particle as the mass of the other particle tends to infinity; it provides the correct isoscalar Z-graph contributions to leading order in  $1/M$  for the  $NN$  system; and the systematic 3D formalism associated with it includes retardation effects without possessing the unphysical singularities that generally are present in quasipotential theories.

For relativistic bound states, the 4D vertex functions at total momentum  $P$  obey

$$\Gamma(P) = U(P)\mathcal{G}_0(P)\Gamma(P). \quad (1.13)$$

Equivalently, one may use the 3D vertex function that is obtained with the use of the ET propagator,

$$\Gamma_{\text{ET}}(P) = U_1(P)\langle\mathcal{G}_0(P)\rangle\Gamma_{\text{ET}}(P). \quad (1.14)$$

Shortly, we shall need the relations of 4D vertex functions to the 3D ones, which is as follows,

$$\Gamma(P) = \Omega^R(P)\Gamma_{\text{ET}}(P), \quad (1.15)$$

where  $\Omega^R$  is defined by,

$$\Omega^R(P) = 1 + [U(P) - U_1(P)]\mathcal{G}_0(P)\Omega^R(P). \quad (1.16)$$

A similar relation is needed for final states:

$$\bar{\Gamma}(P) = \bar{\Gamma}_{\text{ET}}(P)\Omega^L(P), \quad (1.17)$$

$$\Omega^L(P) = 1 + \Omega^L(P)\mathcal{G}_0(P)[U(P) - U_1(P)]. \quad (1.18)$$

In the spirit underlying the use of an effective  $NN$  interaction, the 3D interaction  $U_1$  is truncated at “lowest order” within a systematic expansion in powers of the coupling constant. This truncation violates Lorentz invariance, although the full 3D reduction formalism is equivalent to the 4D formalism and thus respects Lorentz invariance. For electromagnetic matrix elements, the absorption of the virtual photon’s momentum  $Q$  causes the final state to have nonzero three-momentum, even if the initial state did not. Thus, in general, a dynamical boost is needed to obtain wave functions in frames where the bound state has nonzero three-momentum. In our 3D formalism, the dynamical boost is embedded within the equations. Wave functions corresponding to nonzero three-momentum should be obtained straightforwardly by solving the bound-state equation with the interaction appropriate to the moving frame. This differs from the interaction in the c.m. frame because retardation corrections and Dirac spinors in the matrix elements depend upon the total momentum. The violation of Lorentz invariance causes the total bound-state energy  $E(\mathbf{P})$  to differ from  $\sqrt{M_D^2 + \mathbf{P}^2}$ . For the deuteron, the effect is small and it may be compensated by a simple renormalization of the interaction that, in effect, approximately takes into account the terms omitted when  $U_1$  is truncated at lowest order. Results for deuteron form factors have been found in previous calculations to be essentially the same whether the interaction is renormalized or not, thus indicating negligible sensitivity to the truncation and the associated violation of Lorentz invariance.

In order to confront the predictions of this formalism with electron-scattering data we must derive a 3D reduction of the electromagnetic current that is consistent with the reduction of the scattering equation. A clear 4D formalism for the current follows from coupling photons everywhere in the Bethe-Salpeter Green’s function. This leads to the following gauge-invariant 4D result for the photon’s interaction with the two-nucleon system:

$$\mathcal{A}_{\text{BS},\mu} = \bar{\Gamma}(P')G_{0,\mu}^\gamma\Gamma(P) + \bar{\Gamma}(P')G_0(P')K_\mu^\gamma(Q)G_0(P)\Gamma(P), \quad (1.19)$$

where  $P' = P + Q$ ,  $G_{0,\mu}^\gamma$  is a five-point function for insertion of a photon of momentum  $Q$  and Lorentz index  $\mu$  in the free propagator  $G_0$ , and  $K_\mu^\gamma$  is the five-point, two-nucleon irreducible  $NN \rightarrow NN\gamma$  amplitude found by coupling the photon to all charged-particle lines inside the Bethe-Salpeter kernel  $K$ . A similar result holds for the 4D theory involving  $G_C$ ,

$$\mathcal{A}_{\text{ET},\mu} = \bar{\Gamma}(P')\mathcal{G}_{0,\mu}^\gamma\Gamma(P) + \bar{\Gamma}(P')\mathcal{G}_0(P')U_\mu^\gamma(Q)\mathcal{G}_0(P)\Gamma(P), \quad (1.20)$$

where  $\mathcal{G}_{0,\mu}^\gamma = G_{0,\mu}^\gamma + G_{C,\mu}^\gamma$ , and  $U_\mu^\gamma$  is the result of coupling the photon to all internal lines of the reduced interaction  $U$ . In order to develop a conserved current in the 4D theory based on Eq. (1.9), we must construct  $G_{C,\mu}^\gamma$ , which is the extra current required in order that  $\mathcal{G}_{0,\mu}^\gamma$  satisfies a Ward-Takahashi identity involving  $\mathcal{G}_0$ . Unfortunately, this is not straightforward, since in general the variable  $\kappa_2^0$  in  $G_C$  depends on the three-momentum of the intermediate state. As we shall see in Section IV, we cannot simply use the standard fermion electromagnetic current,  $\gamma_\mu$ , since this choice violates current conservation. In Section IV we construct the additional pieces of the current that restore current conservation, thereby obtaining a conserved current  $\mathcal{G}_{0,\mu}^\gamma$  for use with vertex functions obtained from Eq. (1.13).

In this paper, we develop an equivalent 3D form of the current matrix elements for the equal-time formalism, based on an expansion of the formula,

$$\mathcal{A}_{\text{ET},\mu} = \bar{\Gamma}_{\text{ET}}(P') \langle \Omega^L(P') \mathcal{G}_{0,\mu}^\gamma \Omega^R(P) \rangle \Gamma_{\text{ET}}(P) + \bar{\Gamma}_{\text{ET}}(P') \langle \mathcal{G}(P') U_\mu^\gamma \mathcal{G}(P) \rangle \Gamma_{\text{ET}}(P). \quad (1.21)$$

The resultant reduction is consistent with the reduction used to obtain the 3D t-matrix of Eq. (1.11) and the vertex function of Eq. (1.14). Furthermore, this reduction preserves the two-body electromagnetic Ward-Takahashi identities which are present in the 4D theory. Quantities inside angle brackets are integrated over time-components of relative momenta, thus reducing them to a 3D form. This yields a consistent three-dimensional formalism that includes the effects of relativity systematically, has the correct one-body limits, and maintains current conservation. We then apply this machinery to the calculation of electron-deuteron scattering in the impulse approximation.

Previous calculations of electron-deuteron scattering by Hummel and Tjon [15–17] have used instant interactions and a form of the ET current. However, several approximations were employed, such as the use of wave functions based on the 3D quasipotential propagator of Blankenbecler-Sugar [14] and Logunov-Tavkhelidze [7], approximate boost operators, and an electromagnetic current which was conserved only in positive-energy states. Calculations of elastic electron-deuteron scattering also were performed by Devine and Wallace using an instant interaction and the ET propagator of Mandelzweig and Wallace, Eq. (1.12) with the choice of  $\kappa_2^0$  given below that equation. [18] In that work, a suitable conserved current was derived for use with vertex functions that included negative-energy components. In this paper, we extend these previous analyses by use of our systematic 3D formalism with the improved choice of  $\kappa_2^0$  that is needed when retardation effects are included.

It is easy to show that if the instant approximation is used to reduce the four-dimensional equation, Eq. (1.9), to the three-dimensional ET equation, a particularly simple three-dimensional conserved current exists. If we denote this current by  $\mathcal{G}_{\text{inst},\mu}^\gamma$ , then we may write the resulting Ward-Takahashi identity as:

$$Q^\mu \mathcal{G}_{\text{inst},\mu}^\gamma(p_1, p_2; Q) = q_2 [\langle \mathcal{G}_0 \rangle(\mathbf{p}_1, \mathbf{p}_2; P^0) - \langle \mathcal{G}_0 \rangle(\mathbf{p}_1, \mathbf{p}_2 + \mathbf{Q}; P^0 + Q^0)] + (1 \leftrightarrow 2), \quad (1.22)$$

where  $(1 \leftrightarrow 2)$  indicates the part of the current proportional to charge  $q_1$ , with momenta and labels of the two particles interchanged. Consequently, if we construct the current matrix element

$$\mathcal{A}_{\text{inst},\mu} = \int \frac{d^3p}{(2\pi)^3} \bar{\Gamma}_{\text{inst}}(\mathbf{p}; P + Q) \mathcal{G}_{\text{inst},\mu}^\gamma(\mathbf{p}, \mathbf{P}; Q) \Gamma_{\text{inst}}(\mathbf{p}; P), \quad (1.23)$$

where  $\Gamma_{\text{inst}}$  is the vertex function obtained from the bound-state equation corresponding to Eq. (1.14) with an instant interaction chosen for  $U_1$ , then the result will be a conserved impulse current. A similar instant analysis was performed by Devine and Wallace [19]. Our instant calculations differ from those of Ref. [19] in that a slightly different choice for  $\kappa_2^0$  is made than was made by Wallace and Mandelzweig. This different choice for  $\kappa_2^0$  is necessitated by the requirement that the three-dimensional theory with retardations should not possess any unphysical singularities when evaluated in a frame where the two-body system has large momentum.

A first step beyond the instant approximation may be obtained by replacing the vertex  $\Gamma_{\text{inst}}$ , which is calculated with instant OBE interactions, with the vertex  $\Gamma_{\text{ET}}$ , calculated

with the full retarded OBE interaction obtained in the systematic ET formalism. In order to maintain current conservation our approach demands that in making this change we should also replace  $\mathcal{G}_{\text{inst},\mu}^\gamma$  by a significantly more complicated object,  $\mathcal{G}_{0,\mu}^\gamma$ . The resultant current matrix element, which we denote  $\mathcal{A}_{\text{ET},\mu}$ , differs from Eq. (1.23) by replacement of the subscript inst by the subscript ET in the vertex functions and replacement of  $\mathcal{G}_{\text{inst},\mu}^\gamma$  by  $\mathcal{G}_{0,\mu}^\gamma$ . This  $\mathcal{A}_{\text{ET},\mu}$  would satisfy current conservation when retardations are included provided that we also included the two-body currents, such as the one depicted in Figure 2, that become necessary because of retardation effects. This work is concerned primarily with displaying the formalism and performing impulse approximation calculations that explore the effects of retardation and negative-energy components in the vertex functions. Therefore, we use the simpler current  $\langle \mathcal{G}_{\text{inst},\mu}^\gamma \rangle$  with the ET vertex functions as well as with the instant vertex functions. For elastic electron-deuteron scattering this is expected to be a very good approximation to the use of the full ET current. Calculations where  $\langle G_{C,\mu}^\gamma \rangle$  is omitted from the instant current matrix element suggest that the total contribution of  $\langle G_{C,\mu}^\gamma \rangle$  to the observables is small. This is consistent with the interpretation of  $\langle G_{C,\mu}^\gamma \rangle$  as arising from the coupling of the photon to internal charged lines in the crossed-box graph:  $\langle G_{C,\mu}^\gamma \rangle$  is a two-body current, and therefore we would expect it *a priori* to be small at the momentum-transfers under consideration here. Since  $\langle G_{C,\mu}^\gamma \rangle$  itself makes a small contribution to observables, using a form of it that only approximately satisfies current conservation is expected to have an even smaller effect on our numerical results. We expect that these effects, and the other effects of retardations we have neglected in the current, will only have a minor influence on observables. Here our main goal is to examine the effect of retardation on the vertex functions, and the role that negative-energy states play in the calculation, and so we do not calculate these additional effects. Work is in progress to include these extra terms of the current that are derived in Sec. IV in the calculation. We are also calculating meson-exchange currents, such as  $\rho\pi\gamma$  and  $\omega\sigma\gamma$ , which we *do* expect to influence observables.

The first step in obtaining theoretical predictions for the experimental observables in electron scattering on the deuteron is to find the vertex functions  $\Gamma_{\text{inst}}$  and  $\Gamma_{\text{ET}}$ . We take the four-dimensional kernel  $U$  in Eq. (1.9) to be the sum of single-boson exchanges. The parameters for these exchanges are taken from the Bonn-B OBE model, with the exception of the  $\sigma$ -meson coupling, which we leave as a free parameter. From the 4D kernel,  $U_{1,\text{OBE}}$ , an instant interaction,  $U_{1,\text{inst}}$ , is easily found, and a corresponding retarded interaction,  $U_{1,\text{ET}}$ , can be defined by the systematic procedure outlined above. These two different interactions are then inserted into the bound-state equation derived from Eq. (1.14). The  $\sigma$ -meson coupling is adjusted so that the  $NN$  bound-state pole in the  $^3S_1 - ^3D_1$  channel appears at the deuteron mass. Once this is done the deuteron vertex functions  $\Gamma_{\text{inst}}$  and  $\Gamma_{\text{ET}}$  can be extracted. We calculate these two vertex functions including the effects of negative-energy states and also in the approximation where only positive-energy states contribute.

With vertex functions in hand and using the 3D current  $\langle \mathcal{G}_{\text{inst},\mu}^\gamma \rangle$ , we calculate the electron-deuteron scattering observables  $A$ ,  $B$ , and  $T_{20}$ . The results from such a calculation are shown in Figs. 3, 4 and 5. We also show experimental data from Refs. [20–24] for  $A$ , from Refs. [22,23,25,26] for  $B$  and from Refs. [27–32] for  $T_{20}$ . It should be pointed out though, that a number of two-body effects, such as the differences between  $\mathcal{G}_{\text{inst},\mu}^\gamma$  and  $\mathcal{G}_{0,\mu}^\gamma$  that are needed to restore current conservation, and the usual  $\rho\pi\gamma$  MEC contribution, should be added to our calculations before they can be reliably compared to experimental



data. One of the most interesting features is the close similarity of the results based on the ET vertex functions that include retardations and instant vertex functions that do not. We find that once the  $\sigma$  coupling is renormalized at  $Q^2 = 0$  (as must be done to refit the deuteron binding after incorporating the repulsive effects arising from meson retardation), the deuteron properties in these two models are remarkably similar.

For comparison, in Figs. 6, 7 and 8 we display calculations for  $A$ ,  $B$  and  $T_{20}$ , where the effects of negative-energy states are removed. We see that the inclusion of these states in the calculation makes little difference to any of the observables. However, comparing the different positions of the minima in Figs. 4 and 7 we see that including the negative-energy states in the calculation does shift the minimum in  $B$  to somewhat larger  $Q^2$ . A similar effect was observed by van Orden *et al.* [33] in calculations of electron-deuteron scattering using the spectator formalism. However, note that here, in contradistinction to the results of Ref. [33], the inclusion of negative-energy states does *not* bring the impulse approximation calculation into agreement with the data.

The fact that negative-energy states seem to have a smaller effect on observables in the ET analysis than in the spectator analysis of van Orden *et al.* [33] is somewhat surprising. As pointed out above, the ET propagator has twice the negative-energy state propagation amplitude of the Gross propagator. Thus, other differences between the ET and spectator models, not just differences in the role of negative-energy states in the two approaches, appear to be responsible for the differing results for  $B(Q^2)$ . The fact that Ref. [33]’s calculation essentially agrees with the experimental data for  $B(Q^2)$  is not solely attributable to the Gross formalism’s treatment of negative-energy states, since our results show that negative-energy states have a much smaller effect.

We also note that the inclusion of retardation moves the minimum in  $B$  a little higher in  $Q^2$  but otherwise has little observable effect. Again, this additional effect is not enough to bring the predictions of our model into line with the experimental data.

Finally, examining the tensor polarization  $T_{20}$  we see that all the different models produce results which are very similar. This suggests that this observable is fairly insensitive to dynamical details of the deuteron model, at least up to  $Q^2 = 4 \text{ GeV}^2$ .

We find that elimination of the approximations used by Hummel and Tjon produces only minor changes for the experimentally-measured quantities  $A$ ,  $B$ , and  $T_{20}$ , although the precise location of the minimum in the magnetic form factor  $B$  does change when meson retardations are included in the calculation. Nevertheless, there is little improvement in the agreement of the impulse-approximation calculations with the experimental data for  $B$ .

Comparing our results with those of a non-relativistic impulse approximation calculation of the same observables (see, for instance, Ref. [34]) strengthens the conclusion of previous authors that neither the consideration of relativistic kinematics for the nucleons and mesons nor the inclusion of negative-energy state effects improves the agreement with the experimental data. Of course, by definition, such a non-relativistic impulse approximation calculation neglects both relativistic effects and two-body current contributions. Indeed, we see here that, as already found by Arnold *et al.* [34] and Zuilhof and Tjon [35], including relativistic effects actually *worsens* the agreement with the experimental data. The inclusion of these effects to all orders in a  $p/M$  expansion, as done here and in Refs. [34,35] does *not* lead to a small correction which brings the theory into closer agreement with the experimental data. This suggests that the comparative success of a simple non-relativistic impulse approxima-

tion calculation is fortuitous. Dynamical mechanisms beyond the impulse approximation appear to play a more important role in this reaction than one would conclude from the non-relativistic calculation. Figures 3, 4, and 5 imply that once  $Q^2$  gets above about 0.5 GeV<sup>2</sup> two-body current contributions become important. One example of such a two-body current would be meson-exchange current contributions, but it is also possible that other two-body currents are dynamically important in this regime.

The rest of this paper is devoted to a detailed description of our formalism, and to the explanation of technical details pertaining to our calculation that were omitted in the brief sketch of the calculations given here. In Section II we present our modified four-dimensional equation for  $G_C$  with the correct one-body limit and incorporating a form of the eikonal approximation which is an improvement over that proposed in Ref. [1]. The new choice of the parameter  $\kappa_2^0$  has been found to be necessary, when retardations are included in the ET interaction, in order to avoid unphysical singularities when  $\mathbf{P}$  is large. Our formalism for reductions to three dimensions is then used to determine the lowest-order 3D interaction  $U_1$ . In Section III we explain the various interactions that are used in calculations of deuteron wave functions. These can be divided into two classes: instant interactions, and ET interactions that include meson retardation. Within either of these classes, versions of the interactions are constructed that do and do not include the effects of negative-energy states, in order to display the role played by such components of the deuteron wave function. Section IV discusses our 3D reduction of the electromagnetic current that maintains current conservation, including a detailed discussion of the way in which the gauging of the propagator  $G_C$  in our modified four-dimensional equation is performed. The ET current  $\mathcal{G}_{0,\mu}^\gamma$  is derived and we discuss its connection to the simpler current  $\mathcal{G}_{\text{inst},\mu}^\gamma$  that is used in the present calculations. Section V presents details concerning the application of this formalism to the calculation of electromagnetic observables using the wave functions computed as discussed in Section III. Conclusions are presented in Section VI.

## II. BOUND-STATE EQUATIONS WITH CORRECT ONE-BODY LIMITS

### A. A four-dimensional equation

As outlined in the Introduction, a simple four-dimensional equation may be obtained by employing a form of the eikonal approximation to reorganize the generalized ladder Bethe-Salpeter kernel, based upon the fact that we may always write the kernel  $K$  in the iterative form, Eq. (1.8). The question is: what are good choices for  $G_C$  and  $U$ ? To answer this question, consider the lowest order (in coupling constant) parts of the kernels  $K$  and  $U$ . Obviously, the second-order pieces must be the same, i.e.,

$$U^{(2)} = K^{(2)}. \quad (2.1)$$

Meanwhile, at fourth order, we obtain

$$K^{(4)} = U^{(4)} + U^{(2)}G_C U^{(2)}. \quad (2.2)$$

Thus, in order that the expansion for  $U$  can be truncated at second order without losing the one-body limit as  $m_2 \rightarrow \infty$ , the choice of  $G_C$  must be such that the last term captures

the part of  $K^{(4)}$  that is non-zero in that limit. Moreover, if  $G_C$  is chosen in this way, the one-body limit will then be correct no matter the order at which the expansion of  $U$  is truncated.

Consider the fourth-order contribution to  $K$ , i.e., the crossed-box graph depicted (with momentum labels) in Fig. 9. In order to express  $K^{(4)}$  in the form (2.2), it is necessary to commute vertices until they appear in the same order as in  $K^{(2)}G_C K^{(2)}$ . In doing this commutator terms are collected in  $U^{(4)}$ . Once this is done, the part of the graph that takes on an iterative form is expressed as

$$K_{\text{iter}}^{(4)}(k'_1, k'_2; k_1, k_2) = i \int \frac{d^4 p_2}{(2\pi)^4} K^{(2)}(k'_2 - p_2) d_1(P - p_2) d_2(k_2 + k'_2 - p_2) K^{(2)}(p_2 - k_2). \quad (2.3)$$

Here  $K^{(2)}$  is the ladder Bethe-Salpeter kernel,  $P$  is the conserved, total four-momentum:

$$P = k_1 + k_2 = k'_1 + k'_2, \quad (2.4)$$

and the propagators  $d_i$  are given by,

$$d_i(p_i) = \frac{\Lambda_i^+(\mathbf{p}_i)}{p_i^0 - \epsilon_i(\mathbf{p}_i) + i\eta} - \frac{\Lambda_i^-(\mathbf{p}_i)}{p_i^0 + \epsilon_i(\mathbf{p}_i) - i\eta}, \quad (2.5)$$

where

$$\epsilon_i(\mathbf{p}_i) = (\mathbf{p}_i^2 + m_i^2)^{1/2}, \quad (2.6)$$

$$\Lambda_i^\pm(\mathbf{p}_i) = \begin{cases} \frac{1}{2\epsilon_i(\mathbf{p}_i)}, & \text{for spin-zero particles,} \\ \frac{\pm\epsilon_i(\mathbf{p}_i)\gamma^0 - \gamma_i \cdot \mathbf{p}_i + m_i}{2\epsilon_i(\mathbf{p}_i)}, & \text{for spin-half particles,} \end{cases} \quad (2.7)$$

and  $\eta$  is a positive infinitesimal.

In Eq. (2.3) the argument of the function  $d_2$  may be rewritten:

$$(k_2^0 + k_2'^0 - p_2^0, \mathbf{k}_2 + \mathbf{k}'_2 - \mathbf{p}_2). \quad (2.8)$$

Suppose that the zeroth component of the momentum of particle 2 is large. In particular, this will be the case if  $m_2 \gg m_1$  (one-body limit). In this case particle two's intermediate and final-state three-momentum will be largely unaffected by the presence of particle one, and so we may approximate these components as unchanging,

$$\mathbf{k}_2 + \mathbf{k}'_2 \approx 2\mathbf{p}_2. \quad (2.9)$$

This is the eikonal approximation, and it rests upon forward scattering being the dominant mechanism of interaction. Indeed, making the replacement (2.9) in (2.3) will not affect the value of  $K_{\text{iter}}^{(4)}$  in the limit  $m_2 \rightarrow \infty$ .

This argument shows that  $K_{\text{iter}}^{(4)}$  may be approximately rewritten as:

$$K_{\text{iter}}^{(4)}(k'_2, k_2; P) \approx i \int \frac{d^4 p_2}{(2\pi)^4} K^{(2)}(k'_2 - p_2) d_1(P - p_2) d_2(2\kappa_2 - p_2) K^{(2)}(p_2 - k_2), \quad (2.10)$$

with the four-component object  $\kappa_2$  defined by:

$$\kappa_2 = \left( \frac{k_2^0 + k_2'^0}{2}, \mathbf{p}_2 \right). \quad (2.11)$$

In operator notation

$$K_{\text{iter}}^{(4)} \approx K^{(2)} G_C K^{(2)}. \quad (2.12)$$

Now we are in a position to answer the question of how to choose  $G_C$ . Equation (2.10) shows that the choice:

$$G_C(p; P) = id_1(\nu_1 P + p) d_2(2\kappa_2 - \nu_2 P + p), \quad (2.13)$$

which we write symbolically as,

$$G_C = id_1 d_2^c, \quad (2.14)$$

will allow  $U$  to be truncated at second order while still yielding a four-dimensional equation with the correct one-body limit. Here it is understood that when writing  $G_C$  as a function of the four four-momenta  $p'_1, p'_2, p_1$ , and  $p_2$ , we have

$$G_C(p'_1, p'_2; p_1, p_2) = i(2\pi)^8 \delta^{(4)}(p'_1 - p_1) \delta^{(4)}(p'_2 - p_2) d_1(p_1) d_2(2\kappa_2 - p_2). \quad (2.15)$$

On the other hand, in writing Eq. (2.13) we have expressed the result in terms of center-of-mass and relative four-momenta:

$$p_1 = \nu_1 P + p, \quad p_2 = \nu_2 P - p; \quad (2.16)$$

$$\nu_1 = \frac{P^2 + m_1^2 - m_2^2}{2P^2}, \quad \nu_2 = \frac{P^2 - m_1^2 + m_2^2}{2P^2}. \quad (2.17)$$

The propagator  $d_2^c$  defined in (2.13) depends on the zeroth components of the external momenta through the zeroth component of  $\kappa_2$ . Thus the use of operator notation in Eq. (2.12) anticipates a suitable choice for these zeroth components of external momenta.

In the case that particle two is extremely massive, it will not be very far off its mass shell. The total energy  $P^0$  of the system will be approximately the energy of particle two, and thus we choose

$$\kappa_2^0 = \nu_2 P^0. \quad (2.18)$$

This choice was used in Ref. [1] because it leads to an integral equation that satisfies both the criteria needed to obtain the correct one-body limit  $m_2 \rightarrow \infty$ . It also is suitable for equal-mass particles in the center-of-mass frame. However, in frames where the bound state has nonzero total momentum, the choice leads to an interaction that possesses unphysical singularities.

A consideration of the singularities of the interaction when the particles have equal masses suggests that the particles should be equally far off their mass shells in the intermediate state. Hence, in that case we choose

$$\kappa_2^0 = \frac{1}{2} (P^0 - \epsilon_1 + \epsilon_2), \quad (2.19)$$

where, in an arbitrary frame,

$$\epsilon_1 = \epsilon_1(\mathbf{P}/2 + \mathbf{p}); \quad \epsilon_2 = \epsilon_2(\mathbf{P}/2 - \mathbf{p}). \quad (2.20)$$

This choice is consistent with the eikonal approximation and differs from that of Eq. (2.18) only when  $\mathbf{P} \neq 0$ . Note that our new choice for  $\kappa_2^0$  depends not only on the external variables  $P^0$  and  $\mathbf{P}$ , but also on the internal three-momentum  $\mathbf{p}$ . This feature complicates the construction of a conserved current.

Once  $U$  and the  $G_C$  of Eq. (2.13) are chosen, this defines an “improved” ladder BSE, which, in the two-body center-of-mass frame takes the form,

$$\begin{aligned} \Gamma(p'^0, \mathbf{p}'; s) = i \int \frac{d^4 p}{(2\pi)^4} U(p', p) d_1(\nu_1 P^0 + p^0, \mathbf{p}) \\ [d_2(\nu_2 P^0 - p^0, -\mathbf{p}) + d_2(2\kappa_2^0 - \nu_2 P^0 + p^0, -\mathbf{p})] \Gamma(p^0, \mathbf{p}; s). \end{aligned} \quad (2.21)$$

Because the choice of  $\kappa_2^0$  employed here agrees with that of Ref. [1] in the limit  $m_2 \rightarrow \infty$  the proof given there now suffices to show that this equation becomes the appropriate one-body equation in the limit  $m_2 \rightarrow \infty$ . For equal mass particles,  $\kappa_2^0$  is chosen as per Eq. (2.19).

We make the choice (2.19) because it eliminates singularities that afflict the choice (2.18). As observed in Ref. [1] if the choice (2.18) is made for  $\kappa_2^0$  then the equation (2.21) develops a cut beginning at

$$2\nu_2 P^0 = 2m_2 + \mu. \quad (2.22)$$

If we attempt to solve the integral equation (2.21) in a frame moving with large enough three-momentum  $\mathbf{P}$ , then  $P^0 = \sqrt{M_d^2 + \mathbf{P}^2}$  will become big enough to encounter this singularity. However, with the choice (2.19) the interaction does not have this unphysical singularity.

The above arguments pertain to the one-body limit in which  $m_2 \rightarrow \infty$ . Clearly we can interchange the labels on particles one and two in order to obtain a propagator  $id_1^c d_2$  that is motivated by a consideration of the limit  $m_1 \rightarrow \infty$ . In the propagator  $d_1^c$  we choose, for the equal-mass case

$$\kappa_1^0 = \frac{1}{2} (P^0 + \epsilon_1 - \epsilon_2). \quad (2.23)$$

In the case  $m_1 = m_2$ , writing the propagator as in Eq. (2.14) treats the two particles asymmetrically. If they are identical particles this will lead to violations of the identical-particle statistics. To avoid this, we symmetrize the propagator  $G_C$ , by choosing, instead of  $id_1 d_2^c$ , the form

$$\begin{aligned} \mathcal{G}_0 &\equiv G_0 + G_C \\ &= \frac{i}{2} (d_1 + d_1^c)(d_2 + d_2^c). \end{aligned} \quad (2.24)$$

If the mass of particle  $n$  is taken to infinity we use the choice  $\kappa_n^0 = P^0$  in  $d_n^c$ , while the  $\kappa^0$  variable associated with the light particle is chosen to be zero. This yields the one-body

propagator for the light particle, multiplied by a delta function in the relative momentum, and a projection operator onto the positive-energy states of particle  $n$ . Meanwhile, the delta function guarantees that the interaction will be static, and so both conditions necessary for the correct one-body limit to be present are satisfied. However, note that this formal property does not apply to the case of practical interest for this work,  $m_1 = m_2$ , since then  $\kappa_1^0$  and  $\kappa_2^0$  are defined by Eqs. (2.23) and (2.19).

Symbolically we now write our “improved” ladder BSE as

$$\Gamma = U\mathcal{G}_0\Gamma, \quad (2.25)$$

where here, and throughout this work,  $\mathcal{G}_0$  is defined by Eq. (2.24).

We stress that what has been done here is to take certain pieces of the Bethe-Salpeter kernel  $K$  and rewrite them as  $K^{(2)}G_C K^{(2)}$ ,  $K^{(2)}G_C K^{(2)}G_C K^{(2)}$ , etc. Consequently, Eq. (2.25) is equivalent to a Bethe-Salpeter equation in which graphs other than one-meson exchange are approximately included in the kernel. Thus we expect that the solution of this equation may provide a better description of the dynamics of two-particle systems than the ladder BSE amplitude. Numerical calculations in a scalar field theory appear to support this [1].

## B. Summary of the reduction to three dimensions

The 3D reduction that was outlined in the Introduction may now be applied to the 4D equation (2.25). This yields the following 3D equation for the bound-state vertex function,  $\Gamma_{\text{ET}}$ ,

$$\Gamma_{\text{ET}} = U_1 \langle \mathcal{G}_0 \rangle \Gamma_{\text{ET}}, \quad (2.26)$$

with  $\langle \mathcal{G}_0 \rangle$  the three-dimensional propagator of Eq. (1.12), and the interaction  $U_1$  defined as the solution of the following coupled equations,

$$U_1 = \langle \mathcal{G}_0 \rangle^{-1} \langle \mathcal{G}_0 U \mathcal{G} \rangle \langle \mathcal{G}_0 \rangle^{-1}, \quad (2.27)$$

which is three-dimensional, and

$$\mathcal{G} = \mathcal{G}_0 + \mathcal{G}_0(U - U_1)\mathcal{G}. \quad (2.28)$$

Note once more that the solution for  $U_1$  is found by demanding that  $\langle \mathcal{G} \rangle = \langle \mathcal{G}_0 \rangle$ . Equations (2.26) and (2.27) are exactly equivalent to the 4D equation (2.25). Inserting the choice (2.19) for  $\kappa_2^0$  and specializing to the case of equal-mass particles gives

$$\langle \mathcal{G}_0(P) \rangle = \frac{\Lambda_1^+ \Lambda_2^+}{P^0 - \epsilon_1 - \epsilon_2} - \frac{\Lambda_1^+ \Lambda_2^-}{2\epsilon_2} - \frac{\Lambda_1^- \Lambda_2^+}{2\epsilon_1} - \frac{\Lambda_1^- \Lambda_2^-}{P^0 + \epsilon_1 + \epsilon_2}, \quad (2.29)$$

which is a restatement of Eq. (1.12). We note in passing that this is exactly the same expression as that found when the simpler expression  $i\langle d_1(d_2 + d_2^c) \rangle$  is calculated.

By using Eq. (2.26), rather than Eq. (1.2), we not only have a consistent 3D reduction but we approximately include the crossed-ladder graphs, particularly the “Z-graph” contributions where one nucleon is in a positive-energy state and the other is in a negative-energy state.

For equal-mass particles in the center-of-mass frame, Eq. (2.26) agrees with the quasipotential equations of Wallace and Mandelzweig [11]. However, in a quasipotential approach the interaction in other frames should be obtained by boosting via a dynamical equation. This leads to unphysical singularities. The systematic ET formalism avoids these. In essence, the ET formalism with a truncated interaction emphasizes the elimination of unphysical singularities over the strict enforcement of Lorentz invariance.

The second-order 3D interaction  $U_1^{(2)}$  is given by:

$$\langle \mathcal{G}_0 \rangle U_1^{(2)} \langle \mathcal{G}_0 \rangle = \langle \mathcal{G}_0 K^{(2)} \mathcal{G}_0 \rangle \equiv \mathcal{A}. \quad (2.30)$$

An explicit form for  $\mathcal{A}$  can be computed for the case of OBE interactions of the form

$$K^{(2)}(q) = \sum_n \frac{g_n^2 V_n(1) V_n(2)}{q^2 - \mu_n^2} \quad (2.31)$$

where  $V_n(i)$  denotes the appropriate vertex operator for the interaction of the  $n$ th meson with nucleon  $i$ . If we write:

$$\mathcal{A} = \sum_n \sum_{\rho_1 \rho'_1 \rho_2 \rho'_2} \frac{\Lambda_1^{\rho'_1} \Lambda_2^{\rho'_2}}{e'_1 + e'_2} A_n(\rho'_1 \rho'_2 \leftarrow \rho_1 \rho_2) V_n(1) V_n(2) \frac{\Lambda_1^{\rho_1} \Lambda_2^{\rho_2}}{e_1 + e_2}, \quad (2.32)$$

with  $e_i = \rho_i \nu_i \kappa_i^0 - \epsilon_i$ ,  $e'_i = \rho'_i \nu_i \kappa_i'^0 - \epsilon'_i$ ; then, for the exchange of meson  $n$ , the factors  $A_n(\rho'_1 \rho'_2 \leftarrow \rho_1 \rho_2)$  can be written in any rho-spin channel as

$$A_n(\mathbf{p}', \mathbf{p}; P^0, \mathbf{P})(\rho'_1 \rho'_2 \leftarrow \rho_1 \rho_2) = \frac{g_n^2}{8\omega_n} \left[ F(\omega_n + q^0) + F(\omega_n - q^0) \right], \quad (2.33)$$

where

$$\begin{aligned} F(\omega) \equiv & \frac{1}{e_1 + e'_2 - \omega} + \frac{1}{e'_1 + e_2 - \omega} + \frac{1}{e_1 + e'_1 - \omega} + \frac{1}{e_2 + e'_2 - \omega} \\ & + \frac{1}{e_1 + e'_2 - \omega} \left( \frac{e_1 + e_2}{e_2 + e'_2 - \omega} \right) + \frac{1}{e'_1 + e_2 - \omega} \left( \frac{e_1 + e_2}{e_1 + e'_1 - \omega} \right) \\ & + \left( \frac{e'_1 + e'_2}{e_1 + e'_1 - \omega} \right) \frac{1}{e_1 + e'_2 - \omega} + \left( \frac{e'_1 + e'_2}{e_2 + e'_2 - \omega} \right) \frac{1}{e'_1 + e_2 - \omega} \\ & + \frac{e'_1 + e'_2}{e_2 + e'_2 - \omega} \left( \frac{1}{e_1 + e'_2 - \omega} + \frac{1}{e'_1 + e_2 - \omega} \right) \frac{e_1 + e_2}{e_1 + e'_1 - \omega}, \end{aligned} \quad (2.34)$$

and  $q_0 = \kappa_1'^0 - \kappa_1^0$ . The key difference here from the calculation of Ref. [1] is that here the parameter  $\kappa_i^0$  varies with the intermediate-state momentum under consideration. For equal-mass particles

$$\kappa_1^0 = \frac{1}{2} (P^0 + \epsilon_1 - \epsilon_2), \quad \kappa_2^0 = \frac{1}{2} (P^0 - \epsilon_1 + \epsilon_2); \quad (2.35)$$

$$\kappa_1'^0 = \frac{1}{2} (P^0 + \epsilon'_1 - \epsilon'_2), \quad \kappa_2'^0 = \frac{1}{2} (P^0 - \epsilon'_1 + \epsilon'_2). \quad (2.36)$$

The expression for  $\mathcal{A}$  is easily converted into a result for  $U_1^{(2)}$  using the inverse of the propagator  $\langle \mathcal{G}_0 \rangle$ . The result is expressed in terms of matrix elements between initial and final states of any  $\rho$ -spin as follows,

$$U_{1,\text{ET}}^{\rho'_1 \rho'_2, \rho_1 \rho_2}(\mathbf{p}', \mathbf{p}; P^0, \mathbf{P}) = \sum_n \left[ \bar{u}^{\rho'_1}(\rho'_1 \mathbf{p}'_1) V_n(1) u^{\rho_1}(\rho_1 \mathbf{p}_1) \right] \left[ \bar{u}^{\rho'_2}(\rho'_2 \mathbf{p}'_2) V_n(2) u^{\rho_2}(\rho_2 \mathbf{p}_2) \right] \times A_n(\mathbf{p}', \mathbf{p}; P^0, \mathbf{P})(\rho'_1 \rho'_2 \leftarrow \rho_1 \rho_2) \quad (2.37)$$

This is the full ET interaction including retardation effects. If one eliminates the retardation effects, the result is the instant interaction defined by,

$$U_{1,\text{inst}}^{\rho'_1 \rho'_2, \rho_1 \rho_2}(\mathbf{p}', \mathbf{p}; P^0, \mathbf{P}) = \sum_n \left[ \bar{u}^{\rho'_1}(\rho'_1 \mathbf{p}'_1) V_n(1) u^{\rho_1}(\rho_1 \mathbf{p}_1) \right] \left[ \bar{u}^{\rho'_2}(\rho'_2 \mathbf{p}'_2) V_n(2) u^{\rho_2}(\rho_2 \mathbf{p}_2) \right] \left( \frac{-g_n^2}{\omega_n^2} \right). \quad (2.38)$$

Expanding the vertex functions in terms of Dirac spinors,

$$\Gamma_{\text{ET}}(\mathbf{p}, \mathbf{P}) = \gamma_1^0 \gamma_2^0 \sum_{\rho_1 \rho_2} u^{\rho_1}(\rho_1 \mathbf{p}_1) u^{\rho_2}(\rho_2 \mathbf{p}_2) \Gamma_{\text{ET}}^{\rho_1 \rho_2}(\mathbf{p}, \mathbf{P}), \quad (2.39)$$

leads to the coupled equations that we solve,

$$\Gamma_{\text{ET}}^{\rho_1, \rho_2}(\mathbf{p}, \mathbf{P}) = \sum_{\rho'_1 \rho'_2} \int \frac{d^3 p'}{(2\pi)^3} U_1^{\rho_1 \rho_2, \rho'_1 \rho'_2}(\mathbf{p}, \mathbf{p}'; P^0, \mathbf{P}) \langle \mathcal{G}_0 \rangle^{\rho'_1 \rho'_2}(\mathbf{p}', \mathbf{P}) \Gamma_{\text{ET}}^{\rho'_1 \rho'_2}(\mathbf{p}', \mathbf{P}). \quad (2.40)$$

Here the propagator factors  $\langle \mathcal{G}_0 \rangle^{\rho'_1 \rho'_2}$  are  $\langle \mathcal{G}_0 \rangle^{++} = 1/(P^0 - \epsilon'_1 - \epsilon'_2)$ ,  $\langle \mathcal{G}_0 \rangle^{+-} = 1/2\epsilon'_2$ ,  $\langle \mathcal{G}_0 \rangle^{-+} = 1/2\epsilon'_1$  and  $\langle \mathcal{G}_0 \rangle^{--} = -1/(P^0 + \epsilon'_1 + \epsilon'_2)$ .

Two special cases of particular interest are the matrix element of the ET interaction between positive-energy spinors, as follows,

$$U_{1,\text{ET}}^{++,++}(\mathbf{p}', \mathbf{p}; P^0, \mathbf{P}) = \sum_n \left[ \bar{u}^+(\mathbf{p}'_1) V_n(1) u^+(\mathbf{p}_1) \right] \left[ \bar{u}^+(\mathbf{p}'_2) V_n(2) u^+(\mathbf{p}_2) \right] \times \frac{g_n^2}{2\omega_n} \left[ \frac{1}{P^0 - \epsilon'_1 - \epsilon'_2 - \omega_n} + \frac{1}{2} \frac{P^0 - \epsilon_1 - \epsilon_2}{(P^0 - \epsilon'_1 - \epsilon'_2 - \omega_n)^2} + \frac{1}{2} \frac{P^0 - \epsilon'_1 - \epsilon'_2}{(P^0 - \epsilon'_1 - \epsilon'_2 - \omega_n)^2} + \frac{1}{2} \frac{(P^0 - \epsilon'_1 - \epsilon'_2)(P^0 - \epsilon_1 - \epsilon_2)}{(P^0 - \epsilon'_1 - \epsilon'_2 - \omega_n)^3} + (1 \leftrightarrow 2) \right], \quad (2.41)$$

and the matrix element in positive-energy states omitting the effects of  $G_C$ ,

$$U_{1,\text{TOPT}}^{++,++}(\mathbf{p}', \mathbf{p}; P^0, \mathbf{P}) = \sum_n \left[ \bar{u}^+(\mathbf{p}'_1) V_n(1) u^+(\mathbf{p}_1) \right] \left[ \bar{u}^+(\mathbf{p}'_2) V_n(2) u^+(\mathbf{p}_2) \right] \frac{g_n^2}{2\omega_n} \times \left[ \frac{1}{P^0 - \epsilon'_1 - \epsilon'_2 - \omega_n} + (1 \leftrightarrow 2) \right]. \quad (2.42)$$

This is the standard time-ordered perturbation theory (TOPT) one-boson-exchange interaction. Diagrams for the one-pion exchange part of this interaction between positive-energy nucleon states are shown in Fig. 10. There are additional pieces in the ET interaction of Eq. (2.41) that arise from  $G_C$ , i.e., from the approximate inclusion of higher-order graphs in the crossed-ladder kernel, which is necessary to obtain the one-body limits.



### III. CONSTRUCTION OF THREE-DIMENSIONAL NUCLEON-NUCLEON INTERACTIONS

A number of different 3D two-body interactions may be defined by including or not including retardation effects, and by including, or not including the contributions of negative-energy states. These different 3D interactions are used in our assessment of the significance of retardations and of negative-energy states in calculations of electromagnetic observables. In this section we outline the development of the various interactions used in this work, in each case starting from a four-dimensional kernel  $K$  that is the sum of six single-meson exchanges. The mesons are the  $\pi(138)$ , the  $\sigma(550)$ , the  $\eta(549)$ , the  $\rho(769)$ , the  $\omega(782)$ , and the  $\delta(983)$ . The quantum numbers and masses of these mesons, the cutoffs in the (monopole) form factors, as well as the couplings for all but the  $\sigma$  meson, are listed in Table I. All these parameters except for the  $\sigma$  coupling are taken directly from the Bonn-B fit to the  $NN$  phase shifts [36]. The  $\sigma$  coupling is varied so as to achieve the correct deuteron binding energy for each interaction considered.

We then use the techniques of the previous section to construct the following interactions, all of which are to be used in the three-dimensional ET equation (2.40). (Note that in calculating the 3D interaction we assume that the 4D interaction contains no form factors and any dependence of vertex factors  $V_n$  upon  $q^0$  is neglected. After calculating the three-dimensional interaction we then insert monopole form factors at all the vertices.)

1. The “Retarded ET” interaction, given by Eq. (2.37), with the choices (2.23) and (2.19) for  $\kappa_1^0$  and  $\kappa_2^0$ .
2. The instant  $NN$  interaction, defined by Eq. (2.38).
3. The second-order TOPT  $NN$  interaction defined by Eq. (2.42).

The first and second interactions are used in a two-body equation with the full ET Green’s function given by Eq. (2.40), and also in an equation in which only the  $++$  sector is retained. However, for the instant interaction, we follow the practice of Devine and Wallace [18] and switch off by *fiat* couplings that involve flip of both  $\rho$ -spins, i.e., between the  $++$  and  $--$  sectors, and between the  $+-$  and  $-+$  sectors. A partial justification of this rule follows from an analysis of the static limit of our 3D retarded interaction, which shows that all couplings to the  $--$  states vanish as  $1/M \rightarrow 0$ , while other couplings approach the instant form. Although the static limit for coupling of  $+-$  and  $-+$  sectors approaches the standard instant form, we omit this coupling in order to reproduce the previous results of Devine and Wallace.

Since, as we have already discussed, the propagator  $\langle G_0 \rangle^{-1}$  does not exist in the  $+-$  and  $-+$  sectors, the TOPT interaction,  $U_{1,\text{TOPT}}^{++,++}$ , is used with only  $++$  sectors retained in the equation.

Once a particular interaction is chosen, the integral equation (2.40) is solved for the bound-state energy. The method used involves seeking the energy at which the largest eigenvalue of the kernel  $U_1 \langle \mathcal{G}_0 \rangle$  is one. The eigenvalue is calculated using the Malfliet-Tjon iteration procedure. Details of this method, the rho-spin basis chosen, and the way the angular integrations are performed may be found in Ref. [19]. In our calculations we used 40 quadratures in the radial momentum, and 8 in the integration over the polar angle,  $\theta$ . In

the case of the two energy-dependent interactions numerical integration was used to perform the integration over the azimuthal angle,  $\phi$ . We found that 12 quadratures were sufficient to achieve convergence.

In each calculation, the  $\sigma$  coupling was adjusted to get the correct deuteron binding energy, producing the results (accurate to three significant figures) given in Table II. The value given for the instant calculation with positive-energy states alone is that found in the original Bonn-B fit. In all other cases the  $\sigma$  coupling must be adjusted to compensate for the inclusion of retardation, the effects of negative-energy states, etc. We believe that this adjustment of the scalar coupling strength is sufficient to get a reasonable deuteron wave function. However, one direction for future work is to refit the meson-exchange parameters in these various different relativistic  $NN$  interaction models to the  $NN$  scattering data. From Table II we see that (with the exception of the TOPT interaction), adjusting the  $\sigma$  coupling to reproduce the observed deuteron binding leads to at most a 5% deviation from the Bonn-B value, thereby suggesting that other meson parameters would change only slightly if a more detailed fit were performed.

Once the bound-state wave function in the center-of-mass frame has been determined in this fashion, it is a simple matter to solve the integral equation (2.26) in any other frame. As we shall explain below, we choose to calculate electron-deuteron scattering in the Breit frame. Hence, we need to calculate the deuteron wave functions in frames with total four-momentum  $(\sqrt{M_D^2 + \mathbf{P}^2}, \mathbf{P})$ . To do this, the interaction is recalculated in the new frame using the rules given above, and then the integral equation is solved with this new interaction. Because the formalism we use for reducing the four-dimensional integral equation to three dimensions is *not* Lorentz invariant if the potential  $U_1$  is truncated at any finite order in the coupling, we have calculated the eigenvalue  $\lambda(\mathbf{P})$  defined by

$$U_1(\mathbf{P})\langle\mathcal{G}_0(P)\rangle\Gamma_{\text{ET}}(\mathbf{P}) = \lambda(\mathbf{P})\Gamma_{\text{ET}}(\mathbf{P}), \quad (3.1)$$

for each of the five different interactions defined above. Since  $\lambda(\mathbf{0}) = 1$ , by construction, and  $P^0 = \sqrt{M_D^2 + \mathbf{P}^2}$ , is set in accord with Lorentz invariance, the deviation of  $\lambda$  from one indicates the violation of Lorentz invariance in the interaction  $U_1$ . The results of this test are shown in Fig. 11.

Three features of these results are worthy of note. Firstly, for elastic scattering on the deuteron at  $Q \approx 5 \text{ fm}^{-1}$  in the Breit frame, the initial and final states have momenta  $Q/2 \approx 2.5 \text{ fm}^{-1}$  and  $\lambda$  deviates from 1 by only 2% - 3%. Thus for momentum transfers up to of order 1 GeV the violations of Lorentz invariance are actually quite small. Secondly, adding meson retardation to the formalism actually *increases* the violation of Lorentz invariance. This is a little surprising because the retardation effects, when expanded to order  $\mathbf{P}^2/M^2$ , reproduce the Poincaré boost operator of Ref. [37] [1]. We note that if the Poincaré boost operator of order  $\mathbf{P}^2/M^2$  were actually sufficient in this calculation, and effects of higher order in  $1/M$  were truly negligible, then the inclusion of these retardation effects should remove most of the violation of Lorentz invariance present in the instant analysis. This does not happen. Finally, including negative-energy states in the formalism decreases the size of the violation of Lorentz invariance.

## IV. CONSTRUCTION OF A CURRENT-CONSERVING ELECTROMAGNETIC INTERACTION

In this section, we first review how a conserved electromagnetic current is developed for the 4D Bethe-Salpeter formalism, and then show how a corresponding 3D current is obtained from the 4D one. The emphasis is on satisfying the appropriate Ward-Takahashi identities. These reviews establish the procedure that is followed in subsequent subsections in order to construct the electromagnetic current for the 4D and 3D formalisms involving the propagator  $G_C$ . The tricky issue when  $G_C$  is present is the construction of the additional terms in the current to maintain current conservation. Because  $G_C$  enters as a part of two-body interactions associated with crossed graphs, the current associated with it is a two-body current. We construct the extra terms in the current required by the Ward-Takahashi identity, which is not straightforward because the variables  $\kappa_1^0$  and  $\kappa_2^0$  that we choose depend on the three-momentum of the intermediate state. As we shall see below, this means that we cannot use the standard fermion electromagnetic current,  $\gamma_\mu$ , because such a choice would violate current conservation. We show that the Ward-Takahashi identity may be recovered by incorporating an additional term in the current. This yields the ET current referred to as  $\mathcal{G}_{0,\mu}^\gamma$  in the Introduction. We then develop the corresponding 3D current for the formalism involving  $G_C$ . Because the ET current has parts attributable to two-body effects, we also develop a simpler current that is appropriate for use with instant interactions,  $\mathcal{G}_{\text{inst}\mu}^\gamma$ . This last-mentioned current is the one used in the calculations of this paper, which are based upon the impulse approximation. Although we do not use the full formalism developed in this section for calculations in this paper, the results presented here are pertinent to future calculations in which two-body currents will be included.

### A. Review of Ward-Takahashi identities in 4D Bethe-Salpeter formalism

We begin our discussion by reviewing the WTI for the usual Bethe-Salpeter Green's function. Consider the two-body Green's function  $G$  that is the solution of the Bethe-Salpeter equation

$$G = G_0 + G_0 K G, \quad (4.1)$$

where  $K$  is any BSE kernel. Define the two-body Green's function for the interaction of two free particles with a photon of fixed momentum  $Q$  via:

$$\begin{aligned} G_{0,\mu}^\gamma(p_1, p_2, Q) &\equiv G_0(p_1, p_2 + Q)[-ij_\mu^{(2)}(Q^2)d_1^{-1}(p_1)]G_0(p_1, p_2) + (1 \leftrightarrow 2) \\ &= G_{0,\mu}^{\gamma(2)}(p_1, p_2, Q) + G_{0,\mu}^{\gamma(1)}(p_1, p_2, Q). \end{aligned} \quad (4.2)$$

Here, and throughout the rest of the paper, the notation  $(1 \leftrightarrow 2)$  indicates that the momenta of the two particles must be swapped, *and* the labels exchanged. Therefore, the  $(1 \leftrightarrow 2)$  pieces of any expression represent the photon coupling to whichever particle it did not couple in the first part of the expression. An explicit example of this rule is the particle one coupling term of Eq. (4.2), which is  $G_{0,\mu}^{\gamma(1)}(p_1, p_2, Q) = G_0(p_1 + Q, p_2)[-id_2^{-1}(p_2)j_\mu^{(1)}(Q^2)]G_0(p_1, p_2)$ .

The free Green's function  $G_{0,\mu}^\gamma$  obeys a Ward-Takahashi identity. Now let  $G_\mu^\gamma$  be the Green's function for the interaction of one photon with the interacting two-particle system.

Note that in the two-nucleon system the charges  $q_i$  will include isospin operators, so care must be exercised in ordering charges and isospin-dependent interactions. We may write the following equation for a current-conserving  $G_\mu^\gamma$ , by allowing the photon to be inserted anywhere on the right-hand side of Eq. (4.1), and then rearranging the result:

$$G_\mu^\gamma(k'_1, k'_2; k_1, k_2; Q) = \int \frac{d^4 p_1 d^4 p_2}{(2\pi)^8} G(k'_1, k'_2; p_1, p_2 + Q) [-i j_\mu^{(2)}(Q^2) d_1^{-1}(p_1)] G(p_1, p_2; k_1, k_2) \\ + (1 \leftrightarrow 2) + \int \frac{d^4 p'_1 d^4 p'_2 d^4 p_1 d^4 p_2}{(2\pi)^{16}} G(k'_1, k'_2; p'_1, p'_2) K_\mu^\gamma(p'_1, p'_2; p_1, p_2; Q) G(p_1, p_2; k_1, k_2). \quad (4.3)$$

Here  $K_\mu^\gamma$  is found by coupling the photon to every internal charged line in the kernel  $K$ . (Note that there is an overall delta function  $\delta^{(4)}(k'_1 + k'_2 - k_1 - k_2 - Q)$  on both sides of this equation.) Using the WTI for  $G_{0,\mu}^\gamma$ , Eq. (4.3), and the explicit form of Eq. (4.1) we find a WTI for  $G_\mu^\gamma$ ,

$$Q^\mu G_\mu^\gamma(k'_1, k'_2; k_1, k_2; Q) = q_2 G(k'_1, k'_2 - Q; k_1, k_2) - G(k'_1, k'_2; k_1, k_2 + Q) q_2 + (1 \leftrightarrow 2), \quad (4.4)$$

provided that

$$q_2 K(p'_1, p'_2 - Q; p_1, p_2) - K(p'_1, p'_2; p_1, p_2 + Q) q_2 + (1 \leftrightarrow 2) = Q^\mu K_\mu^\gamma(p'_1, p'_2; p_1, p_2; Q), \quad (4.5)$$

which is the WTI for the interaction current. (Similar identities are used in the construction of Ward-Takahashi identities for the Gross—or spectator—formalism in Refs. [38,39].) The result (4.5) is completely general, and will always hold if the two-body current  $K_\mu^\gamma$  is constructed by coupling the photon to every charged line in the kernel  $K$ .

Using the usual decomposition of the two-body Green's function into a pole and a regular part gives the amplitude for interaction of the bound-state with a photon of momentum  $Q$  [40]. Expressing the result in terms of total and relative four-momenta yields:

$$\mathcal{A}_\mu(P, Q) = \int \frac{d^4 p}{(2\pi)^4} \bar{\Gamma}(p - Q/2; P') G_{0,\mu}^{\gamma(2)}(p; P; Q) \Gamma(p; P) + (1 \leftrightarrow 2) \\ + \int \frac{d^4 p' d^4 p}{(2\pi)^8} \bar{\Gamma}(p'; P') G_0(p'; P') K_\mu^\gamma(p', P'; p, P; Q) G_0(p; P) \Gamma(p; P), \quad (4.6)$$

where  $P' = P + Q$  and  $\Gamma(p; P)$  is the two-body vertex function corresponding to the bound-state at four-momentum  $P^2 = M^2$ . From the WTIs for  $G_{0,\mu}^\gamma$  and  $K_\mu^\gamma$ , and the bound-state BSE,  $\Gamma = K G_0 \Gamma$ , it is then straightforward to show that

$$Q^\mu \mathcal{A}_\mu(P, Q) = 0, \quad (4.7)$$

as required for current conservation.

## B. Gauge invariance in a 3D reduction of the Bethe-Salpeter formalism

In the context of a reduction to three dimensions, the question is how to maintain gauge invariance when the reduction is made. In Section I we outlined the 3D reduction method

for the bound-state vertex arising from the solution of the Bethe-Salpeter equation. This gives

$$\Gamma_1(P) = K_1(P)\langle G_0(P)\rangle\Gamma_1(P), \quad (4.8)$$

where the dependence of quantities on the total four momentum,  $P$ , is indicated. The 4D vertex function,  $\Gamma$ , and the corresponding 3D one,  $\Gamma_1$ , are related as follows,

$$G_0(P)\Gamma(P) = \mathcal{G}(P)\Gamma_1(P). \quad (4.9)$$

Moreover, the interaction  $K_1$  is defined so as to obey,

$$\langle G_0(P)\rangle K_1(P)\langle G_0(P)\rangle = \langle G_0(P)K(P)\mathcal{G}(P)\rangle. \quad (4.10)$$

Inserting Eq. (4.9) into Eq. (4.6), we find an entirely equivalent expression for the current,

$$\begin{aligned} \mathcal{A}_\mu(P, Q) = & \int \frac{d^4k' d^4p' d^4p d^4k}{(2\pi)^{16}} \bar{\Gamma}_1(\mathbf{k}'; P') \mathcal{G}(k', p'; P') \\ & \left[ -ij_\mu^{(1)}(Q^2)d_2^{-1}(\nu_2 P - p)\delta^{(4)}(p' - p - Q/2) - ij_\mu^{(2)}(Q^2)d_1^{-1}(\nu_1 P + p)\delta^{(4)}(p' - p + Q/2) \right. \\ & \left. + K_\mu^\gamma(P', p'; P, p; Q) \right] \mathcal{G}(p, k; P)\Gamma_1(\mathbf{k}; P). \end{aligned} \quad (4.11)$$

Because the vertex functions do not depend upon the time-components of relative momenta, integrations over  $k^0$  and  $k^{0'}$  reduce this expression to a 3D one, which we abbreviate as

$$\mathcal{A}_\mu = \bar{\Gamma}_1(P')\langle \mathcal{G}(P') \left[ J_\mu + K_\mu^\gamma \right] \mathcal{G}(P) \rangle \Gamma_1(P). \quad (4.12)$$

Now, given a result for  $\Gamma_1$  obtained by systematic expansion of  $K_1$ , the amplitude  $\mathcal{A}_\mu$  also can be expanded systematically in a way that maintains current conservation. First, note that we solve for  $K_1$  in accord with Eq. (4.10). This leads to an infinite series for  $K_1$ . If the condition (4.10) is imposed order-by-order in the expansion in  $K - K_1$ , the condition defines  $K_1$  to the same order. Truncation of the kernel is necessary for a practical analysis and we must ask if a corresponding 3D approximation for the current matrix element (4.12) exists that maintains the Ward-Takahashi identities of the theory. *It turns out that the current matrix element (4.12) is conserved if  $\mathcal{G}(J_\mu + K_\mu^\gamma)\mathcal{G}$  on the right-hand side of Eq. (4.12) is expanded to a given order in the coupling constant and the kernel  $K_1$  used to define  $\Gamma_1$  is obtained from Eq. (4.10) by truncation at the same order in the coupling constant.*

To effect this the right-hand side of Eq. (4.12) is split into two pieces, one due to the one-body current  $J_\mu$ , and one due to the two-body current  $K_\mu^\gamma$ . Suppose now that  $K_1$  has been truncated at lowest order, i.e.,  $K_1 = K_1^{(2)}$ , and that  $K_\mu^\gamma = K_\mu^{\gamma(2)}$ . Then, in the  $J_\mu$  piece, we expand the  $\mathcal{G}$ s and retain terms up to the same order in  $K^{(2)} - K_1^{(2)}$ . A piece from the two-body current must be added to this. In that piece we stop this expansion of  $\mathcal{G}$  at zeroth order in  $K^{(2)} - K_1^{(2)}$ , i.e., write  $\mathcal{G} = G_0$ . Thus, we define our second-order approximation to  $\mathcal{A}_\mu$ ,  $\mathcal{A}_\mu^{(2)}$ , by

$$\begin{aligned} \mathcal{A}_\mu^{(2)} = & \bar{\Gamma}_1(P')\langle G_{0\mu}^\gamma \rangle \Gamma_1(P) \\ & + \bar{\Gamma}_1(P')\langle G_0(P')(K^{(2)}(P') - K_1^{(2)}(P'))G_{0\mu}^\gamma \rangle \Gamma_1(P) \\ & + \bar{\Gamma}_1(P')\langle G_{0\mu}^\gamma(K^{(2)}(P) - K_1^{(2)}(P))G_0(P) \rangle \Gamma_1(P) \\ & + \bar{\Gamma}_1(P')\langle G_0(P')K_\mu^{\gamma(2)}G_0(P) \rangle \Gamma_1(P). \end{aligned} \quad (4.13)$$

To show that  $\mathcal{A}_\mu^{(2)}$  is gauge invariant, it must be contracted with the four-vector  $Q$ . The WTIs for  $G_{0\mu}^\gamma$ ,  $K_\mu^\gamma$ , together with the bound-state equation (4.8), can be used to show that

$$\begin{aligned} Q^\mu \mathcal{A}_\mu^{(2)} = & -\bar{\Gamma}_1(P') \langle G_0(P') (K^{(2)}(P') - K_1^{(2)}(P')) G_0(P') \rangle q_1 \Gamma_1(P) \\ & + \bar{\Gamma}_1(P') q_1 \langle G_0(P) (K^{(2)}(P) - K_1^{(2)}(P)) G_0(P) \rangle \Gamma_1(P) + (1 \leftrightarrow 2). \end{aligned} \quad (4.14)$$

Thus, at second-order in the coupling constant, with Eq. (4.10) expanded at second order defining  $K_1^{(2)}$ , the corresponding amplitude for electromagnetic interactions of the bound state, as defined by Eq. (4.13), obeys

$$Q^\mu \mathcal{A}_\mu^{(2)} = 0. \quad (4.15)$$

It is straightforward to check that the same result holds if Eq. (4.10) for  $K_1$  is truncated at fourth order, while the one-body and two-body current pieces of Eq. (4.11) similarly are expanded to fourth order. This defines a vertex function  $\mathcal{A}_\mu^{(4)}$  which obeys  $Q^\mu \mathcal{A}_\mu^{(4)} = 0$ . Thus, truncating the kernel  $K_1$  defined by Eq. (4.10) and the electromagnetic vertex defined by Eq. (4.12) at consistent order in the coupling constant yields a current-conserving electromagnetic matrix element. A covariant extension of the formalism presented here is given in Ref. [2].

In fact,  $\mathcal{A}_\mu^{(2)}$  includes contributions from diagrams where the photon couples to particles one and two while exchanged quanta are “in-flight”. These contributions are of two kinds. Firstly, if the four-dimensional kernel  $K$  is dependent on the total momentum, or if it involves the exchange of charged particles, then gauge invariance requires the presence of terms representing the coupling of the photon to internal lines in  $K$ . Secondly, even if gauge invariance does not require the presence of such terms in the four-dimensional formalism, terms arise in the three-dimensional formalism where the photon couples to particles one and two while an exchanged particle is “in-flight”. These must be included if our approach is to contain a WTI. (See Fig. 2 for a diagrammatic interpretation of one such term.)

A special case of the above results occurs when retardation effects are omitted, i.e., the kernel  $K_1 = K_{\text{inst}}$ , is chosen, and the bound-state equation (1.2) is solved to get the vertex function  $\Gamma_1 = \Gamma_{\text{inst}}$ . Then a gauge-invariant current is obtained by implementing the instant approximation in the expression (4.13) in a way consistent with that in which it was used in obtaining the Salpeter equation (1.2). Taking Eq. (4.13) and imitating the derivation of the Salpeter equation by replacing  $K$  by  $K_{\text{inst}}$  leads to

$$\mathcal{A}_{\text{inst},\mu}(P, Q) = \bar{\Gamma}_{\text{inst}}(P') \langle G_{0\mu}^\gamma \rangle \Gamma_{\text{inst}}(P) + \bar{\Gamma}_{\text{inst}}(P') \langle G_0(P') \rangle K_{\text{inst}\mu}^\gamma \langle G_0(P) \rangle \Gamma_{\text{inst}}(P), \quad (4.16)$$

where we have also replaced the meson-exchange current kernel  $K_\mu^\gamma$  by the instant approximation thereto. By definition this instant meson-exchange current kernel obeys the WTI (4.5), but with the instant kernel  $K_{\text{inst}}$  appearing on the right-hand side. To show that Eq. (4.16) defines a gauge-invariant matrix element we contract with the four vector  $Q^\mu$  and use the Ward-Takahashi identities for  $J_\mu$  and  $K_{\text{inst}\mu}^\gamma$ . This gives:

$$\begin{aligned} Q^\mu \mathcal{A}_{\text{inst},\mu}(P, Q) = & \bar{\Gamma}_{\text{inst}}(P') q_2 \langle G_0(P) - G_0(P') \rangle \Gamma_{\text{inst}}(P) \\ & + \bar{\Gamma}_{\text{inst}}(P') \langle G_0(P') (q_2 K_{\text{inst}}(P) - K_{\text{inst}}(P') q_2) G_0(P) \rangle \Gamma_{\text{inst}}(P) + (1 \leftrightarrow 2). \end{aligned} \quad (4.17)$$

Using the bound-state equation,  $\Gamma_{\text{inst}} = K_{\text{inst}} \langle G_0 \rangle \Gamma_{\text{inst}}$ , both at total momentum  $P$  and at total momentum  $P'$  then gives the desired WTI:

$$Q^\mu \mathcal{A}_{\text{inst},\mu}(P, Q) = 0. \quad (4.18)$$

Note that if the four-dimensional interaction  $K$  does not depend on the total momentum  $P$  then the simple current

$$\mathcal{A}_{\text{inst},\mu}(P, Q) = \bar{\Gamma}_{\text{inst}}(P') \langle G_{0,\mu}^\gamma(P; Q) \rangle \Gamma_{\text{inst}}(P), \quad (4.19)$$

is gauge invariant.

### C. Gauge invariance in the 4D formalism with $G_C$

In this section we construct a conserved current for the 4D equation

$$\Gamma = U \mathcal{G}_0 \Gamma. \quad (4.20)$$

In order to do this we rewrite the equation as two coupled equations, the first of which involves the Bethe-Salpeter kernel  $K$ ,

$$\Gamma = K G_0 \Gamma, \quad (4.21)$$

and the second of which defines the reduced interaction  $U$ ,

$$K = U + U G_C K. \quad (4.22)$$

From Eq. (4.6) we see that the gauge-invariant current for the photon coupling to the bound state will contain a piece corresponding to the coupling of photon lines in all possible ways inside  $K$ . This piece of the current is composed of two parts, as follows,

$$K_\mu^\gamma = (1 + K G_C) U_\mu^\gamma (1 + G_C K) + K G_{C,\mu}^\gamma K. \quad (4.23)$$

The Ward-Takahashi identities that are required to be satisfied involve one for  $U_\mu^\gamma$  that takes the same form as Eq. (4.5), with  $K$  replaced by  $U$ .

$$q_2 U(p'_1, p'_2 - Q; p_1, p_2) - U(p'_1, p'_2; p_1, p_2 + Q) q_2 + (1 \leftrightarrow 2) = Q^\mu U_\mu^\gamma(p'_1, p'_2; p_1, p_2; Q). \quad (4.24)$$

The other involves the Green's function  $G_{C,\mu}^\gamma$ , representing a photon coupling to the propagator  $G_C$ . This piece must be constructed in accordance with the Ward-Takahashi identity:

$$Q^\mu G_{C,\mu}^\gamma(p_1, p_2, Q) = q_2 (G_C(p_1, p_2) - G_C(p_1, p_2 + Q)) + (1 \leftrightarrow 2). \quad (4.25)$$

When both of the WTI's (4.24) and (4.25) hold, then the electromagnetic kernel  $K_\mu^\gamma$  will satisfy the WTI (4.5). In this case the current appropriate to a photon insertion in the free propagator is

$$\mathcal{G}_{0,\mu}^\gamma \equiv G_{0,\mu}^\gamma + G_{C,\mu}^\gamma, \quad (4.26)$$

and so, if  $\Gamma$  obeys Eq. (4.20), the amplitude

$$\begin{aligned} \mathcal{A}_\mu(P, Q) = & \int \frac{d^4 p}{(2\pi)^4} \bar{\Gamma}(p - Q/2; P') \mathcal{G}_{0,\mu}^{\gamma(2)}(p; P; Q) \Gamma(p; P) + (1 \leftrightarrow 2) \\ & + \int \frac{d^4 p' d^4 p}{(2\pi)^8} \bar{\Gamma}(p'; P') \mathcal{G}_0(p'; P') U_\mu^\gamma(p', P'; p, P; Q) \mathcal{G}_0(p; P) \Gamma(p; P), \end{aligned} \quad (4.27)$$

will satisfy the current conservation condition (4.7).

In order to implement this formalism, we must construct a current  $G_{C\mu}^\gamma$  that obeys Eq. (4.25). Rather than immediately tackling the full  $G_C$  defined by Eq. (2.24) we first perform this task for one term by considering the simple case in which the propagator is  $id_1 d_2^c$  and the photon couples only to particle two. This is non-trivial because the choice of variable  $\kappa_2^0$  in  $d_2^c$  in general depends on the three-momenta of both particles. For instance, if  $\kappa_2^0$  is chosen as in Eq. (2.19) and the particles are of equal mass then the  $\kappa_2^0$  which appears in the propagator  $G_C(p_1, p_2 + Q)$  is (for equal-mass particles)

$$\kappa_2^{0'} = \frac{1}{2}(P_0 + Q_0 - \epsilon_1 + \epsilon'_2), \quad (4.28)$$

where  $P \equiv p_1 + p_2$ , and  $\epsilon'_2 = \epsilon_2(\mathbf{p}_2 + \mathbf{Q})$ . This is to be compared to the case where  $\kappa_2^0$  is defined via Eq. (2.18). In that case the  $\kappa_2^0$  appearing in  $G_C(p_1, p_2 + Q)$  is, for equal mass particles,

$$\kappa_2^{0'} = \frac{1}{2}(P_0 + Q_0), \quad (4.29)$$

and there is thus no dependence on the intermediate-state three-momenta of particles one and two. As we shall see below, the appearance of momenta in the choice (4.28) for  $\kappa_2^0$  leads to complications in the construction of a current obeying (4.25).

To construct such a current, we first postulate the form

$$d_{c,\mu}^{\gamma(2)}(p_2; Q) \equiv d_2^{\tilde{c}}(p_2 + Q) j_{c,\mu}^{(2)} d_2^c(p_2), \quad (4.30)$$

where we write  $d_2^{\tilde{c}}$  in order to indicate that the constraint on  $\kappa_2^0$  is different once the photon strikes particle two. The WTI for this current is then:

$$Q^\mu j_{c,\mu}^{(2)} = q_2(d_2^{\tilde{c}}(p_2 + Q)^{-1} - d_2^c(p_2)^{-1}). \quad (4.31)$$

Constructing the right-hand side of this equation, for spin-half particles we obtain

$$q_2 [2(\not{\kappa}_2' - \not{\kappa}_2) - \not{Q}] \quad (4.32)$$

Using the form for  $\kappa_2$ , Eq. (2.11), and three-momentum conservation,  $\mathbf{p}_2' = \mathbf{p}_2 + \mathbf{Q}$ , we see that

$$d_2^{\tilde{c}}(p_2 + Q)^{-1} - d_2^c(p_2)^{-1} = [2(\kappa_2^{0'} - \kappa_2^0) - 2Q^0] \gamma_2^0 + \not{Q}. \quad (4.33)$$

Note that if we make the choice (2.18) then,  $\kappa_2^{0'}$  is given by  $\kappa_2^{0'} = \nu_2(P^0 + Q^0)$  and  $\kappa_2^0 = \nu_2 P^0$ , so



$$d_2^{\tilde{c}}(p_2 + Q)^{-1} - d_2^c(p_2)^{-1} = \not{Q} + 2(\nu_2 - 1)Q^0\gamma_2^0. \quad (4.34)$$

This means that, in the Breit frame where  $Q^0 = 0$ , the usual current  $j_\mu^{(2)} = q_2\gamma_{2\mu}$  satisfies the Ward-Takahashi identity (4.31).

However, when we use the formulae (4.28) and (2.19) in the case of equal-mass particles, note that

$$2(\kappa_2^{0'} - \kappa_2^0) = Q^0 + \frac{\mathbf{Q} \cdot (\mathbf{p}_2' + \mathbf{p}_2)}{\epsilon_2 + \epsilon_2'}, \quad (4.35)$$

thus implying that

$$d_2^{\tilde{c}}(p_2 + Q)^{-1} - d_2^c(p_2)^{-1} = \not{Q} - Q \cdot \frac{\hat{p}_2' + \hat{p}_2}{\epsilon_2' + \epsilon_2} \gamma_{20}, \quad (4.36)$$

where  $\hat{p}_2' = (\epsilon_2', \mathbf{p}_2')$ ,  $\hat{p}_2 = (\epsilon_2, \mathbf{p}_2)$ . Consequently, the WTI (4.31) requires that we define the current

$$j_{c,\mu}^{(2)} = q_2\gamma_\mu - \tilde{j}_\mu^{(2)}, \quad (4.37)$$

where

$$\tilde{j}_\mu^{(2)} = q_2 \frac{\hat{p}_{2\mu}' + \hat{p}_{2\mu}}{\epsilon_2' + \epsilon_2} \gamma_{20}, \quad (4.38)$$

is the additional piece of the current that compensates for the dependence of  $\kappa_2^0$  on momentum. Note that  $j_{c,0}^{(2)} = 0$  with this choice of  $j_{c,\mu}^{(2)}$ . Note also the identity

$$Q^\mu \tilde{j}_\mu^{(2)} = 2(\kappa_1^{0'} - \kappa_1^0)q_2\gamma_{20}. \quad (4.39)$$

Next we consider a second piece of  $G_C$ , namely the propagator  $id_1^c d_2$ , still in the situation where the photon couples only to particle two. Denote the free  $NN \rightarrow NN\gamma$  Green's function corresponding to this situation by  $d_\mu^{\tilde{c}}$ . The Ward-Takahashi identity which this Green's function should obey is,

$$Q^\mu d_\mu^{\tilde{c}}(p_1, p_2; Q) = iq_2[d_1^c(p_1)d_2(p_2) - d_1^{\tilde{c}}(p_1)d_2(p_2 + Q)]. \quad (4.40)$$

Note that here the propagator  $d_1^{\tilde{c}}(p_1) \neq d_1^c(p_1)$ , since the change in the momentum of particle two after the impact of the photon leads to a change in the choice of  $\kappa_1^0$  that appears in  $d_1^{\tilde{c}}$ —in spite of particle one apparently being a spectator in this interaction. Again, the simplest choice

$$d_\mu^{\tilde{c}}(p_1, p_2; Q) = id_1^c(p_1)d_2(p_2 + Q)q_2\gamma_{2\mu}d_2(p_2) \quad (4.41)$$

does not obey the Ward-Takahashi identity. However, if we construct  $d_\mu^{\tilde{c}}$  according to

$$\begin{aligned} d_\mu^{\tilde{c}}(p_1, p_2; Q) = & \frac{i}{2} \left[ (d_1^c(p_1) + d_1^{\tilde{c}}(p_1))d_2(p_2 + Q)q_2\gamma_{2\mu}d_2(p_2) \right. \\ & \left. + d_1^{\tilde{c}}(p_1)\tilde{j}_{2\mu}\gamma_2^0\gamma_1^0d_1^c(p_1)(d_2(p_2 + Q) + d_2(p_2)) \right] \end{aligned} \quad (4.42)$$

then it does obey the WTI (4.40). This can be shown as follows. Contracting the right-hand side of Eq. (4.42) with  $Q^\mu$  gives

$$\begin{aligned} \frac{i}{2} \Big[ & (d_1^c(p_1) + d_1^{\tilde{c}}(p_1))q_2(d_2(p_2) - d_2(p_2 + Q)) \\ & + d_1^{\tilde{c}}(p_1)q_2 2(\kappa_1^{0'} - \kappa_1^0)\gamma_1^0 d_1^c(p_1)(d_2(p_2 + Q) + d_2(p_2)) \Big]. \end{aligned}$$

But,

$$2(\kappa_1^{0'} - \kappa_1^0)\gamma_{10} = d_1^{\tilde{c}}(p_1)^{-1} - d_1^c(p_1)^{-1}, \quad (4.43)$$

and so, the Green's function defined by Eq. (4.42) does indeed satisfy the WTI (4.40).

It is now possible to combine the results for  $j_{c,\mu}^{(2)}$  and  $d_\mu^{\tilde{c}}$  in order to construct the 4D current  $\mathcal{G}_{0,\mu}^\gamma = G_{0,\mu}^\gamma + G_{C,\mu}^\gamma$  corresponding to the free Green's function (2.24). In this case the relevant WTI (again, only writing explicitly the parts where the photon couples to particle two) is:

$$\begin{aligned} Q^\mu \mathcal{G}_{0,\mu}^\gamma(p_1, p_2; Q) = & \frac{i}{2} q_2 (d_1(p_1) + d_1^c(p_1))(d_2(p_2) + d_2^c(p_2)) \\ & - \frac{i}{2} q_2 (d_1(p_1) + d_1^{\tilde{c}}(p_1))(d_2(p_2 + Q) + d_2^{\tilde{c}}(p_2 + Q)) + (1 \leftrightarrow 2). \end{aligned} \quad (4.44)$$

Using the forms already constructed for  $j_{2\mu}^c$  and  $d_\mu^{\tilde{c}}$  we discover that the 4D current in the formalism involving  $G_C$  is:

$$\begin{aligned} \mathcal{G}_{0,\mu}^\gamma(p_1, p_2; Q) = & \frac{i}{4} \Big[ (2d_1(p_1) + d_1^c(p_1) + d_1^{\tilde{c}}(p_1))(d_2(p_2 + Q)q_2\gamma_{2\mu}d_2(p_2) + d_2^{\tilde{c}}(p_2 + Q)j_{c,\mu}^{(2)}d_2^c(p_2)) \\ & + d_1^{\tilde{c}}(p_1)\tilde{j}_{2\mu}\gamma_2^0\gamma_1^0d_1(p_1)(d_2(p_2) + d_2(p_2 + Q) + d_2^c(p_2) + d_2^{\tilde{c}}(p_2 + Q)) \Big] + (1 \leftrightarrow 2), \end{aligned} \quad (4.45)$$

and it obeys Eq. (4.44).

## D. Reduction to 3D and the ET current

Having constructed a 4D current for the formalism involving  $G_C$  that obeys the required Ward-Takahashi identity, we can apply the reduction formalism of Section IV B to obtain the currents corresponding to the 3D reduction of this 4D theory. To this end, we first note that the 4D vertex functions are related to 3D ones,  $\Gamma_{\text{ET}}$ , by Eqs. (1.15) and (1.17). Using these relations to rewrite the 4D current (1.21) in terms of the 3D vertex functions shows that

$$\begin{aligned} \mathcal{A}_{\text{ET},\mu} = & \bar{\Gamma}_{1,\text{ET}}(P') \langle \Omega^L(P') \mathcal{G}_{0,\mu}^\gamma \Omega^R(P) \rangle \Gamma_{1,\text{ET}}(P) \\ & + \bar{\Gamma}_{1,\text{ET}}(P') \langle \mathcal{G}(P') U_\mu^\gamma \mathcal{G}(P) \rangle \Gamma_{1,\text{ET}}(P). \end{aligned} \quad (4.46)$$

Here,  $U_\mu^\gamma$  denotes the interaction current obtained by coupling the photon in all possible ways within the reduced interaction  $U$ . In the same manner as discussed for the 3D version of

the Bethe-Salpeter current, it is possible to maintain gauge invariance if the 3D interaction  $U_1$  is truncated at some definite order in the coupling constant, while the expansions for  $\Omega^L \mathcal{G}_{0,\mu}^\gamma \Omega^R$  and  $\mathcal{G} U_\mu^\gamma \mathcal{G}$  similarly are truncated at the same order in the coupling constant.

Because we truncate our effective interaction at second order, the corresponding conserved current in 3D form is obtained by use of  $\Omega^{R(2)} = 1 + [U^{(2)} - U_1^{(2)}] \mathcal{G}_0$  and a corresponding expansion for  $\Omega^{L(2)}$  in Eq. (4.46). The result for the 3D current,

$$\begin{aligned} \mathcal{A}_\mu^{(2)} = & \bar{\Gamma}_{1,\text{ET}}(P') \langle \mathcal{G}_{0,\mu}^\gamma \rangle \Gamma_{1,\text{ET}}(P) \\ & + \bar{\Gamma}_{1,\text{ET}}(P') \langle \mathcal{G}_0(P') (U^{(2)}(P') - U_1^{(2)}(P')) \mathcal{G}_{0,\mu}^\gamma \rangle \Gamma_{1,\text{ET}}(P) \\ & + \bar{\Gamma}_{1,\text{ET}}(P') \langle \mathcal{G}_{0,\mu}^\gamma (U^{(2)}(P) - U_1^{(2)}(P)) \mathcal{G}_0(P) \rangle \Gamma_{1,\text{ET}}(P) \\ & + \bar{\Gamma}_{1,\text{ET}}(P') \langle \mathcal{G}_0(P') U_\mu^{\gamma(2)} \mathcal{G}_0(P) \rangle \Gamma_{1,\text{ET}}(P), \end{aligned} \quad (4.47)$$

obeys the Ward-Takahashi identity (4.15).

Note that  $U^{(2)} = K^{(2)}$  and  $U_\mu^{\gamma(2)} = K_\mu^{\gamma(2)}$  are correct at second order in expansions in the coupling constant. Consequently if we are considering one-boson exchange interactions the only contributions to  $K_\mu^{\gamma(2)}$  that are necessary for gauge invariance come from the photon coupling to isovector exchange particles and from contact terms due to derivative couplings of the mesons to the nucleon. Since these give rise to isovector structures their contribution to electromagnetic scattering off the deuteron is, in fact, zero.

### E. Impulse-approximation current based on the instant approximation to ET formalism

Just as in the case of the Bethe-Salpeter equation, if the instant approximation is used to obtain from Eq. (2.25) the three-dimensional equation that defines the vertex function, then a corresponding gauge-invariant impulse current can be constructed by replacing  $U$  by  $U_{\text{inst}}$  everywhere in the expression (4.47). Assuming that the interaction in the four-dimensional equation does not depend on the total momentum, this leads to a particularly simple conserved current:

$$\mathcal{A}_{\text{inst},\mu} = \bar{\Gamma}_{\text{inst}} \langle \mathcal{G}_{0,\mu}^\gamma \rangle \Gamma_{\text{inst}}. \quad (4.48)$$

At this point it appears that we must integrate the rather complicated formula (4.45) over the zeroth component of relative momentum in order to calculate  $\langle \mathcal{G}_{0,\mu}^\gamma \rangle$ . However, the result (4.45) for  $\mathcal{G}_{0,\mu}^\gamma$  was constructed in order to obey Ward-Takahashi identities in the full four-dimensional theory. It is not, in fact, necessary to use the full result if we are only concerned with maintaining WTIs at the three-dimensional level in the instant approximation. As remarked following Eq. (1.12), the simpler propagator  $\langle d_1(d_2 + d_2^c) \rangle$  provides the same result as  $\langle \mathcal{G}_0 \rangle$ . Thus, we may construct the corresponding current

$$\mathcal{G}_{\text{inst},\mu}^\gamma(\mathbf{p}_1, \mathbf{p}_2; P, Q) = i \langle d_1(p_1) d_2(p_2 + Q) j_\mu^{(2)} d_2(p_2) + d_1(p_1) d_2^c(p_2 + Q) j_{c,\mu}^{(2)} d_2^c(p_2) \rangle + (1 \leftrightarrow 2). \quad (4.49)$$

When contracted with  $Q^\mu$  this gives

$$Q^\mu \mathcal{G}_{\text{inst},\mu}^\gamma(p_1, p_2; Q) = iq_2[\langle d_1(p_1)d_2(p_2) \rangle - \langle d_1(p_1)d_2(p_2 + Q) \rangle + \langle d_1(p_1)d_2^c(p_2) \rangle - \langle d_1(p_1)d_2^c(p_2 + Q) \rangle] + (1 \leftrightarrow 2) \quad (4.50)$$

$$= q_2[\langle \mathcal{G}_0 \rangle(\mathbf{p}_1, \mathbf{p}_2; P^0) - \langle \mathcal{G}_0 \rangle(\mathbf{p}_1, \mathbf{p}_2 + \mathbf{Q}; P^0 + Q^0)] + (1 \leftrightarrow 2). \quad (4.51)$$

Consequently if a vertex function  $\Gamma_{\text{inst}}$  is constructed to be a solution to Eq. (2.26) then the current matrix element defined by

$$\mathcal{A}_{\text{inst},\mu} = \int \frac{d^3p}{(2\pi)^3} \bar{\Gamma}_{\text{inst}}(\mathbf{p} - \mathbf{Q}/2; P') \mathcal{G}_{\text{inst},\mu}^{\gamma(2)}(\mathbf{p}, \mathbf{P}; Q) \Gamma_{\text{inst}}(\mathbf{p}; P) + (1 \leftrightarrow 2), \quad (4.52)$$

obeys the current conservation condition (4.18). The current  $\mathcal{G}_{\text{inst},\mu}^\gamma$  is simpler than the full ET current and omits only effects stemming from retardation in the current. Since our present calculations are designed to provide an assessment of the role of negative-energy states and retardation effects in the vertex functions, and these effects stemming from retardation in the current are expected to be minor,  $\mathcal{G}_{\text{inst},\mu}^\gamma$  is used in these calculations.

## V. ELECTRON-DEUTERON SCATTERING: IMPULSE APPROXIMATION CALCULATIONS

Now we are in a position to calculate the deuteron electromagnetic form factors  $A$  and  $B$ , and the tensor polarization  $T_{20}$ . These are related to the charge, quadrupole, and magnetic form factors of the deuteron,  $F_C$ ,  $F_Q$ , and  $F_M$ , by the following formulae,

$$A = F_C^2 + \frac{8}{9}\eta^2 F_Q^2 + \frac{2}{3}\eta F_M^2, \quad (5.1)$$

$$B = \frac{4}{3}\eta(1 + \eta)F_M^2, \quad (5.2)$$

$$t_{20} = -\sqrt{2} \frac{x(x+2) + y/2}{1 + 2(x^2 + y)}; \quad (5.3)$$

where

$$x = \frac{2\eta F_Q}{3F_C}, \quad (5.4)$$

$$y = \frac{2\eta}{3} \left[ \frac{1}{2} + (1 + \eta) \tan^2 \left( \frac{\theta_e}{2} \right) \right] \left( \frac{F_M}{F_C} \right)^2, \quad (5.5)$$

$$\eta = -\frac{Q^2}{4M_D^2}; \quad (5.6)$$

where  $Q^2$  is the square of the four-momentum transfer. For elastic electron-deuteron scattering,  $Q$  is space-like and  $\eta$  is positive. In this work all plots and data are quoted at an electron angle of  $\theta_e = 70$  degrees.

Deuteron form factors  $F_C$ ,  $F_Q$ , and  $F_M$  are related to the matrix elements of the current  $\mathcal{A}_\mu$  discussed in the previous section, taken between the three different magnetic quantum number states  $|M\rangle = | +1\rangle$ ,  $|0\rangle$ , and  $| -1\rangle$  of the deuteron as follows:

$$F_C = \frac{1}{3\sqrt{1+\eta}e}(\langle 0|\mathcal{A}^0|0\rangle + 2\langle +1|\mathcal{A}^0|+1\rangle), \quad (5.7)$$

$$F_Q = \frac{1}{2\eta\sqrt{1+\eta}e}(\langle 0|\mathcal{A}^0|0\rangle - \langle +1|\mathcal{A}^0|+1\rangle), \quad (5.8)$$

$$F_M = \frac{-1}{\sqrt{2\eta(1+\eta)}e}\langle +1|\mathcal{A}_+|0\rangle. \quad (5.9)$$

Matrix elements of  $\mathcal{A}_\mu$  are calculated in the Breit frame, with kinematics as shown in Fig. 12. In order to calculate matrix elements such as those defined by Eq. (4.52) we require the vertex functions, or equivalently the wave functions, in the frame where the total four-momentum is  $P = (\sqrt{M_D^2 + \mathbf{Q}^2/4}, \mathbf{Q}/2)$ . However, these are precisely the wave functions calculated in Section III. Thus, we now take the wave functions constructed for the five different interactions of Section III at  $\mathbf{P}^2$  ranging from 0 to 25 fm<sup>-2</sup> and insert them into the expression (4.52). The explicit form of the three-dimensional current  $\mathcal{G}_{\text{inst},\mu}^\gamma$  is presented in Appendix B. In using any of the interactions obtained with only positive-energy state propagation we of course drop all pieces of the operator  $\mathcal{G}_{\text{inst},\mu}^\gamma$  in negative-energy state sectors.

The general form of a matrix element of the operator  $\mathcal{A}_\mu$ , using the deuteron vertex-function decomposition developed in Ref. [19], is, for coupling only to particle one,

$$\begin{aligned} \langle M'|\mathcal{A}_\mu|M\rangle = \int \frac{d^3p}{(2\pi)^3} [\Gamma_1^{\rho'_1 s'_1 \rho_2 s_2, M'}(\mathbf{p} + \mathbf{Q}/2, P + Q)]^* \langle \mathcal{G}_0 \rangle^{\rho'_1 \rho_2}(\mathbf{p} + \mathbf{Q}/2; P + Q) \\ J_{1,\mu}^{\rho'_1 s'_1 \rho_1 s_1 \rho_2 s_2} \langle \mathcal{G}_0 \rangle^{\rho_1 \rho_2}(\mathbf{p}; P) \Gamma_1^{\rho_1 s_1 \rho_2 s_2, M}(\mathbf{p}; P) + (1 \leftrightarrow 2), \end{aligned} \quad (5.10)$$

with:

$$\langle \mathcal{G}_0 \rangle^{\rho_1 \rho_2}(\mathbf{p}; P) \equiv \rho_1 \rho_2 \frac{1}{\frac{1}{2}(\rho_1 + \rho_2)P^0 - \epsilon_1 - \epsilon_2 + \frac{1}{2}(\rho_1 - \rho_2)(\epsilon_1 - \epsilon_2)}, \quad (5.11)$$

and

$$J_{1,\mu}^{\rho'_1 s'_1 \rho_1 s_1 \rho_2 s_2} = \rho_2 \bar{u}^{\rho'_1 s'_1}(\rho'_1 \mathbf{p}'_1) \hat{J}_{1,\mu}^{\rho'_1 \rho_1 \rho_2} u^{\rho_1 s_1}(\rho_1 \mathbf{p}_1), \quad (5.12)$$

where the form of  $\hat{J}_{1,\mu}^{\rho'_1 \rho_1 \rho_2}$  is rho-spin dependent and is given in Appendix B.

The single-nucleon currents used in these calculations are the usual one for extended nucleons, defined for  $n = 1$  or 2 by

$$j^{(n),\mu} = q_n \left( \gamma_n^\mu F_1^{(n)}(Q^2) + \frac{i}{2M_N} \sigma_n^{\mu\nu} Q_\nu F_2^{(n)}(Q^2) \right). \quad (5.13)$$

The appearance of the factor  $F_1$  in the first term here implies that the WTI  $Q^\mu j_\mu = 0$  is not satisfied. On the other hand, as pointed out by Gross and Riska a current which obeys the original WTI is

$$j_{WT}^\mu = \gamma^\mu + \frac{1}{2M_N} \sigma^{\mu\nu} Q_\nu F_2(Q^2) + [F_1(Q^2) - 1] \left[ \gamma^\mu - Q^\mu \frac{\gamma^\nu Q_\nu}{Q^2} \right]. \quad (5.14)$$

The difference between  $j^\mu$  and  $j_{WT}^\mu$  is proportional to  $Q^\mu$ . Therefore, for elastic electron-deuteron scattering in the Breit frame only  $j^3$  will be affected if we adopt the WTI-obeying current  $j_{WT}^\mu$  instead of the original extended-nucleon current  $j^\mu$ . Recall that in the Breit frame  $j^3$  is formally constrained by current conservation to be proportional to  $j^0$ , and is never evaluated. Hence, it transpires that by formally adding a piece to the one-body current  $j^\mu$  we can obtain a one-body current for an extended object which still satisfies  $Q^\mu j_\mu = \mathcal{Q}$ , and yet, in this calculation, leads to the same numerical results as Eq. (5.13). We choose to parametrize the single-nucleon form factors  $F_1$  and  $F_2$  via the 1976 Höhler fits [41]. Choosing different single-nucleon form factors does not affect our qualitative conclusions, although it has some impact on our quantitative results for  $A$ ,  $B$ , and  $T_{20}$ .

Using such a one-body current the calculation described above conserves the electromagnetic current if the vertex function  $\Gamma_1$  is obtained using an instant potential. However, in all other circumstances it violates the Ward-Takahashi identities by omission of pieces that are required because of the inclusion of retardation effects in the calculation. This violation of the WTI's comes from two sources.

Firstly, in, for instance, the TOPT calculation, the pieces of the current coming from terms in Eq. (4.13) of the form

$$\langle G_0(P')(K^{(2)} - K_1^{(2)})G_0(P)J_\mu G_0(P) \rangle$$

are not included if Eq. (4.52) is applied. The inclusion of these “in-flight” contributions to the current in our calculations, and the consequent restoration of current conservation in the TOPT calculation, will be the subject of a future paper. There these contributions, and meson-exchange current effects such as the  $\rho\pi\gamma$  and  $\omega\sigma\gamma$  MECs will be calculated. Of course, similar “in-flight” pieces are missing from the “retarded ET” calculation.

Secondly, even if these “in-flight” pieces are included in the retarded ET calculation the WTI's will not hold. Pieces will still be missing from the current (4.52). Specifically, we need to use the more complicated form of  $\mathcal{G}_{0,\mu}^\gamma$  given in Eq. (4.45). However, calculations where  $\langle G_{C,\mu}^\gamma \rangle$  is omitted from the instant current matrix element suggest that the total contribution of  $\langle G_{C,\mu}^\gamma \rangle$  to the observables is small. Since  $\langle G_{C,\mu}^\gamma \rangle$  itself makes a small contribution to observables, using a form of it that only approximately satisfies current conservation is expected to have an even smaller effect on our numerical results.

## VI. CONCLUSION

The ET formalism developed here provides a systematic three-dimensional theory of electromagnetic interactions involving relativistic bound states. This is achieved by integrating over time components of relative momenta. For the propagator of the theory, this produces a form corresponding to zero relative time of the two particles. In order for this formalism to incorporate the Z-graphs that are expected in a quantum field theory, it is necessary for the propagator to include terms that come from crossed Feynman graphs. The predominant terms that are needed have been derived using a form of the eikonal approximation. This leads to the ET propagator. In this paper, we discuss a refined version of the ET propagator involving a different choice of  $\kappa_2^0$  from that of Refs. [10,11]. This new choice of  $\kappa_2^0$  avoids the unphysical singularities which otherwise occur in the three-dimensional ET interaction when it is evaluated in a frame where the bound state has large three-momentum.

Given a suitable choice for the ET propagator, one may calculate the interaction and the electromagnetic currents that must be used with it. A full accounting of both the couplings to negative-energy states and the role of retardations in the interaction is thereby obtained.

When the electromagnetic currents are constructed in our 3D theory the necessary Ward-Takahashi identities are clearly satisfied provided that one calculates both the interaction and the electromagnetic current to all orders. However, this is neither practical, nor, if an effective hadronic Lagrangian is being used, desirable. A truncation of both the interaction and the electromagnetic current is needed. It is not *a priori* evident that one may truncate the expansion for the both the interaction and the electromagnetic current in a way that systematically maintains current conservation. We show that this can in fact be done in the ET formalism.

Violations of Lorentz invariance occur when the interaction is truncated. For the range of momenta that arise in electron deuteron scattering at TJNAF  $Q^2$  these violations may be compensated for by the use of a renormalized interaction. It is found that the required renormalization typically is no more than a few percent. Based upon this, we do not expect this violation of Lorentz invariance to have a significant effect on results for electron-deuteron scattering.

Calculations have been performed for the impulse approximation, in which we use an instant approximation for the electromagnetic current. This current satisfies current conservation when used with deuteron vertex functions that are obtained with instant interactions. We also have used this simple current with vertex functions that include the full retardations obtained in the ET formalism.

Impulse approximation results fall systematically below experimental data for the form factors  $A$  and  $B$  for  $Q > 3\text{--}4\text{ fm}^{-1}$ . This deficiency of the theoretical calculations at higher  $Q$  indicates that additional mechanisms beyond the impulse approximation should be significant. However, the existing tensor polarization data are reasonably well described, and this is consistent with previous analyses that have shown  $T_{20}$  to be less sensitive to two-body currents.

The role of negative-energy states is found to be not very large. Our impulse-approximation numerical results are in closer agreement with those of Hummel and Tjon [15–17] than with those based upon the spectator formalism [33]. Because the ET formalism incorporates the relevant Z-graphs in a preferable way, we are confident that Z-graphs play a minor role in calculations that are based upon standard boson-exchange models of the  $NN$  interaction. The role of retardation corrections in the deuteron vertex functions also is rather minor.

Further calculations are needed in order to incorporate the full ET current and the meson-exchange currents.

## ACKNOWLEDGMENTS

We thank the U. S. Department of Energy for its support under grant no. DE-FG02-93ER-40762. D. R. P. is grateful for the warm hospitality of the Special Research Centre for the Subatomic Structure of Matter, where the writing of this paper was completed.

## APPENDIX A: LEADING EFFECTS IN $1/M$ OF TIME-ORDERED Z-GRAPHS

Here we examine the fourth-order graphs for the  $NN$  t-matrix in the equal-time formalism and show that the contributions of order  $1/M$  are correctly reproduced in the ET equation with instant interactions.

The fourth-order piece of the equal-time Green's function is:

$$\langle G_0 K^{(2)} G_0 K^{(2)} G_0 \rangle + \langle G_0 K^{(4)} G_0 \rangle \quad (\text{A1})$$

where  $K$  is the full Bethe-Salpeter kernel. If we consider only positive-energy states on the external lines, and decompose the internal nucleon lines according to the different rho-spins which are possible, we produce forty-eight graphs. However, if we restrict our attention to graphs which contribute at order  $1/M$  or above only the twelve graphs shown in Fig. 13 are relevant. Of these, those on the first and third lines arise from the first, iterative, part of expression (A1) while those on the second and fourth line come from the crossed-box piece of Eq. (A1).

The external Green's functions are now amputated, and the static limit of

$$T_{++\rightarrow++}^{(4)} = \langle G_0 \rangle_{++}^{-1} \left[ \langle G_0 K^{(2)} G_0 K^{(2)} G_0 \rangle + \langle G_0 K^{(4)} G_0 \rangle \right]_{++\rightarrow++} \langle G_0 \rangle_{++}^{-1} \quad (\text{A2})$$

is taken. In this limit the first two graphs in Fig. 13 are infinitely enhanced, as they come from the iteration of the lowest-order interaction  $K_1^{(2)}$ . Meanwhile the next four graphs give energy denominators:

$$-\frac{1}{\omega_1} \frac{1}{\omega_1 + \omega_2} \frac{1}{\omega_2} - \frac{1}{\omega_2} \frac{1}{\omega_1 + \omega_2} \frac{1}{\omega_1} - 2 \frac{1}{\omega_1} \frac{1}{\omega_1 + \omega_2} \frac{1}{\omega_1}, \quad (\text{A3})$$

where  $\omega_1$  ( $\omega_2$ ) is the energy of the first (second) meson emitted from nucleon one. These graphs do not vanish in the limit  $M \rightarrow \infty$ . They correspond to a shorter-range interaction than  $K_1^{(2)}$ , and are formally part of the fourth-order three-dimensional kernel  $K_1^{(4)}$ . Their effects are usually subsumed into  $K_1^{(2)}$  through the fitting of the parameters in that interaction to the  $NN$  scattering data.

The contribution of the remaining six graphs begins at order  $1/M$ . At that order they give energy denominators

$$\begin{aligned} & -\frac{1}{\omega_1} \frac{1}{2M} \frac{1}{\omega_2} - \frac{1}{2M} \frac{1}{\omega_1 + \omega_2} \frac{1}{\omega_2} - \frac{1}{\omega_1} \frac{1}{\omega_1 + \omega_2} \frac{1}{2M} \\ & - \frac{1}{\omega_2} \frac{1}{2M} \frac{1}{\omega_1} - \frac{1}{2M} \frac{1}{\omega_1 + \omega_2} \frac{1}{\omega_1} - \frac{1}{\omega_2} \frac{1}{\omega_1 + \omega_2} \frac{1}{2M}. \end{aligned} \quad (\text{A4})$$

Including the appropriate spinors and factors to obtain the full expression shows that the sum of these graphs yields:

$$g^4 \bar{u}_1^+ V_1(1) u_1^- \bar{u}_2^+ V_1(2) u_2^+ \bar{u}_1^- V_2(1) u_1^+ \bar{u}_2^+ V_2(2) u_2^+ \left( -\frac{1}{\omega_1^2} \right) \left( -\frac{1}{2M} \right) \left( -\frac{1}{\omega_2^2} \right), \quad (\text{A5})$$

where  $V_i(j)$  is the vertex for the interaction of meson  $i$  with nucleon  $j$ . Note that in writing this expression we have taken some liberties with the ordering of these vertices. However,



the error that this produces is of higher order in  $1/M$ . To order  $1/M$  Eq. (A5) reproduces the  $++ \rightarrow ++$  matrix element of the iteration of the instant interaction using the  $-+$  sector of the ET propagator:

$$\bar{u}_1^+ \bar{u}_2^+ K_{\text{inst}}^{(2)} \frac{\Lambda_1^- \Lambda_2^+}{-2M} K_{\text{inst}}^{(2)} u_1^+ u_2^+. \quad (\text{A6})$$

Similarly, the  $1 \leftrightarrow 2$  version of expression (A6) gives the six fourth-order particle-two Z-graphs correctly to order  $1/M$ .

Thus we see that using the ET propagator with an instant interaction correctly reproduces the  $1/M$  pieces of the fourth-order Z-graphs in the scattering series. By contrast, the Gross or BSLT propagator with an instant interaction would yield a fourth-order Z-graph contribution which is only half the correct size.

## APPENDIX B: EXPLICIT FORM OF THE IMPULSE APPROXIMATION CURRENT

In this appendix we present the explicit form of the impulse approximation current which yields a current-conserving calculation if vertices obtained using an instant interaction are considered. Recall that

$$\mathcal{G}_{\text{inst},\mu}^\gamma(\mathbf{p}_1, \mathbf{p}_2; P, Q) = i \langle d_1(p_1 + Q) j_\mu^{(1)} d_1(p_1) d_2(p_2) + d_1^c(p_1 + Q) j_{c,\mu}^{(1)} d_1^c(p_1) d_2(p_2) \rangle + (1 \leftrightarrow 2). \quad (\text{B1})$$

Inserting the forms of the propagators and performing the integrals over relative momenta we arrive at a form which is most easily expressed in terms of the quantity  $\hat{J}_\mu^{\rho_1 \rho_2}$ , as written in Eq. (5.10). In rho-spin conserving sectors it is:

$$\hat{J}_\mu^{\rho_1 \rho_2} = j_\mu - (1 - \delta_{\rho_1 \rho_2}) \tilde{j}_\mu, \quad (\text{B2})$$

where  $\tilde{j}_\mu$  is the object defined for nucleon two in Eq. (4.38). In our calculation the  $\tilde{j}_\mu$  defined there is multiplied by  $F_1(Q^2)$  in order to take into account the extended-nucleon structure. Likewise,  $j_\mu$  is the usual extended-nucleon current (5.13).

Meanwhile, in rho-spin changing sectors we have:

$$\begin{aligned} \hat{J}_\mu^{-++} = & \left[ 1 - 2 \frac{\kappa_2^{0'} - \epsilon_2}{Q^0 + \epsilon_1 + \epsilon_1'} + \frac{P^0 - \epsilon_1 - \epsilon_2}{Q^0 + \epsilon_1 + \epsilon_1'} + \frac{P^0 - \epsilon_1 - \epsilon_2}{Q^0 + 2(\kappa_1^0 - \kappa_1^{0'}) - \epsilon_1 - \epsilon_1'} \right] j_\mu \\ & - \frac{P^0 - \epsilon_1 - \epsilon_2}{Q^0 + 2(\kappa_1^0 - \kappa_1^{0'}) - \epsilon_1 - \epsilon_1'} \tilde{j}_\mu \end{aligned} \quad (\text{B3})$$

$$\begin{aligned} \hat{J}_\mu^{+-+} = & \left[ 1 + 2 \frac{\kappa_2^0 - \epsilon_2}{Q^0 - \epsilon_1 - \epsilon_1'} - \frac{P^{0'} - \epsilon_1' - \epsilon_2}{Q^0 + 2(\kappa_1^0 - \kappa_1^{0'}) + \epsilon_1 + \epsilon_1'} - \frac{P^{0'} - \epsilon_1' - \epsilon_2}{Q^0 - \epsilon_1 - \epsilon_1'} \right] j_\mu \\ & + \frac{P^{0'} - \epsilon_1' - \epsilon_2}{Q^0 + 2(\kappa_1^0 - \kappa_1^{0'}) + \epsilon_1 + \epsilon_1'} \tilde{j}_\mu \end{aligned} \quad (\text{B4})$$

$$\hat{J}_\mu^{-+-} = \left[ 1 + 2 \frac{\kappa_2^0 + \epsilon_2}{Q^0 + \epsilon_1 + \epsilon_1'} - \frac{P^{0'} + \epsilon_1' + \epsilon_2}{Q^0 + 2(\kappa_1^0 - \kappa_1^{0'}) - \epsilon_1 - \epsilon_1'} - \frac{P^{0'} + \epsilon_1' + \epsilon_2}{Q^0 + \epsilon_1 + \epsilon_1'} \right] j_\mu$$

$$+ \frac{P^{0'} + \epsilon'_1 + \epsilon_2}{Q^0 + 2(\kappa_1^0 - \kappa_1^{0'}) - \epsilon_1 - \epsilon'_1} \tilde{j}_\mu \quad (\text{B5})$$

$$\begin{aligned} \hat{j}_\mu^{+-} = & \left[ 1 - 2 \frac{\kappa_2^{0'} + \epsilon_2}{Q^0 - \epsilon_1 - \epsilon'_1} + \frac{P^0 + \epsilon_1 + \epsilon_2}{Q^0 - \epsilon_1 - \epsilon'_1} + \frac{P^0 + \epsilon_1 + \epsilon_2}{Q^0 + 2(\kappa_1^0 - \kappa_1^{0'}) + \epsilon_1 + \epsilon'_1} \right] j_\mu \\ & - \frac{P^0 + \epsilon_1 + \epsilon_2}{Q^0 + 2(\kappa_1^0 - \kappa_1^{0'}) + \epsilon_1 + \epsilon'_1} \tilde{j}_\mu \quad (\text{B6}) \end{aligned}$$

These reduce to the formulae of Devine [18] if the appropriate limits are taken. Note that in  $++$  states the current  $\hat{J}_\mu$  is just the usual single-nucleon current (5.13).

# TABLES

TABLE I. Meson quantum numbers, masses, cutoffs, and couplings as taken from the Bonn-B model. Note that the number in brackets in the  $\rho$  row is the  $\rho$ -meson tensor coupling.

Meson	$J^P$	$T$	Mass (MeV)	Cutoff (MeV)	$g^2/4\pi$
$\pi$	$0^-$	1	138.03	1200	14.6
$\eta$	$1^-$	0	548.8	1500	5.0
$\rho$	$1^+$	1	769.0	1300	0.95 (6.1)
$\omega$	$1^+$	0	782.6	1500	20.0
$\delta$	$0^+$	1	983.0	1500	3.1155
$\sigma$	$0^+$	0	550.0	2000	

TABLE II. Sigma coupling required to produce the correct deuteron binding energy in the five different models under consideration here.

Interaction	States included	$g_\sigma^2/4\pi$
Instant	$++$	8.08
Klein	$++$	9.64
Retarded ET	$++$	8.39
Instant ET	All	8.55
Retarded ET	All	8.44

# FIGURES

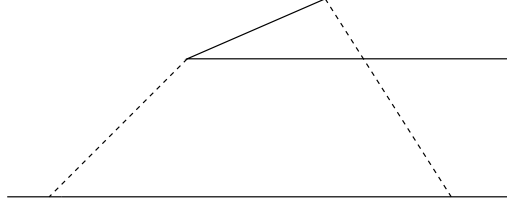


FIG. 1. One example of a Z-graph which is not included in the ladder Bethe-Salpeter equation scattering series

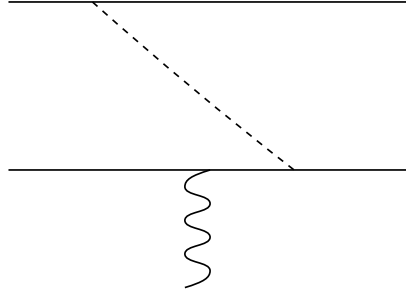


FIG. 2. One example of a two-body current that is required in our formalism in order to maintain gauge invariance.

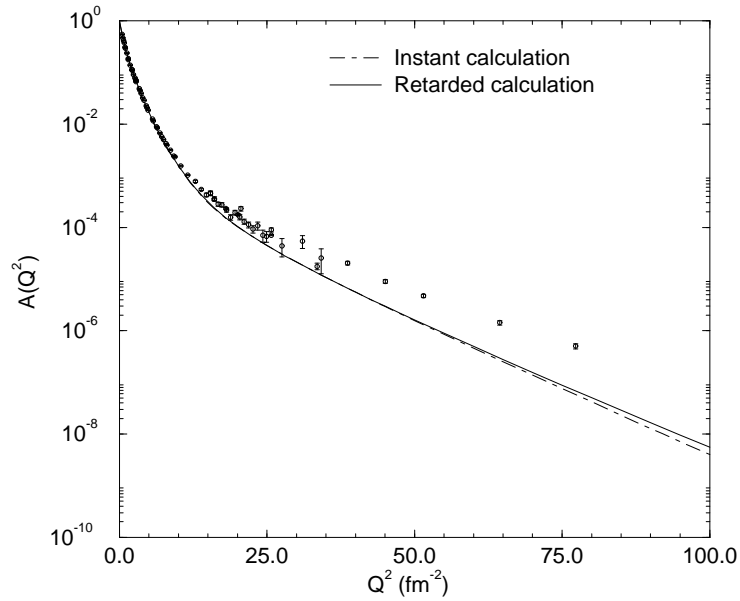


FIG. 3. The form factor  $A(Q^2)$  for the deuteron. The dash-dotted line represents a calculation using a vertex function generated using the instant interaction. Meanwhile the solid line is the result obtained with the retarded ET vertex function. In both cases both positive and negative-energy sectors are included.

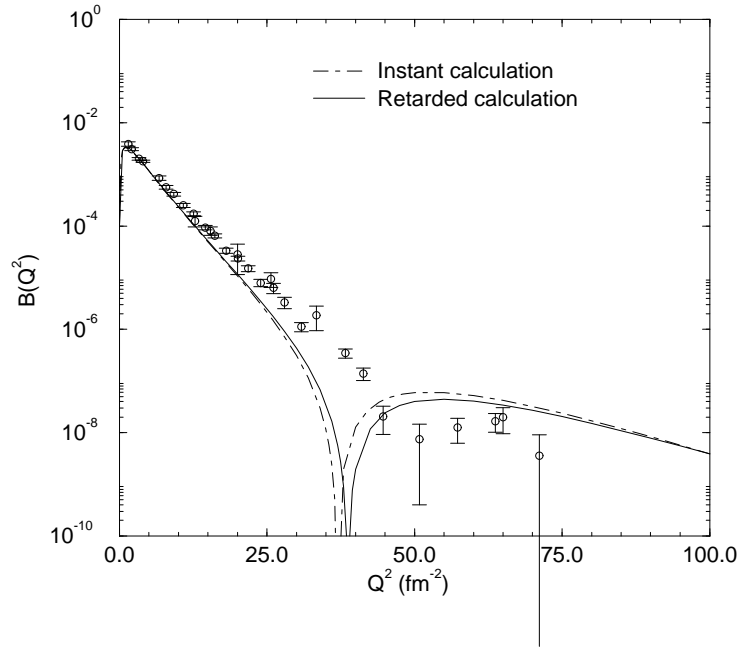


FIG. 4. The form factor  $B(Q^2)$  for the deuteron, legend as in Fig. 3.

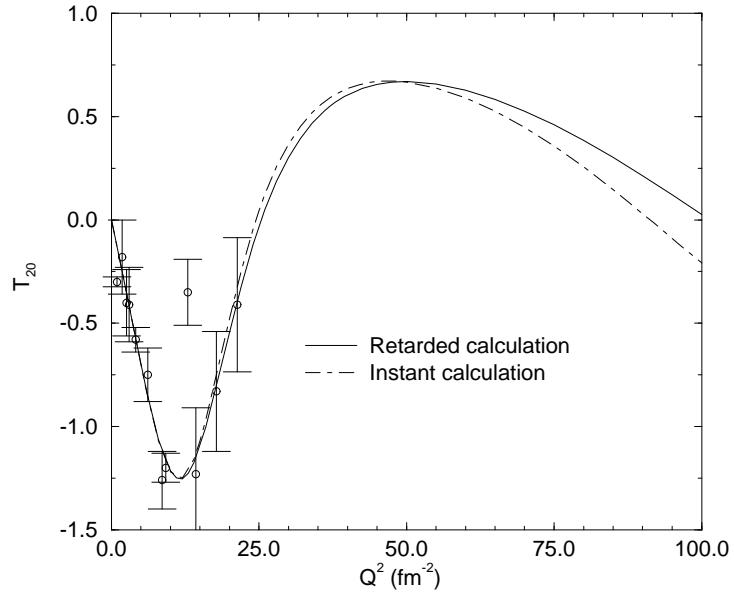


FIG. 5. The tensor polarization  $T_{20}(Q^2)$  in electron-deuteron scattering, legend as in Fig. 5.

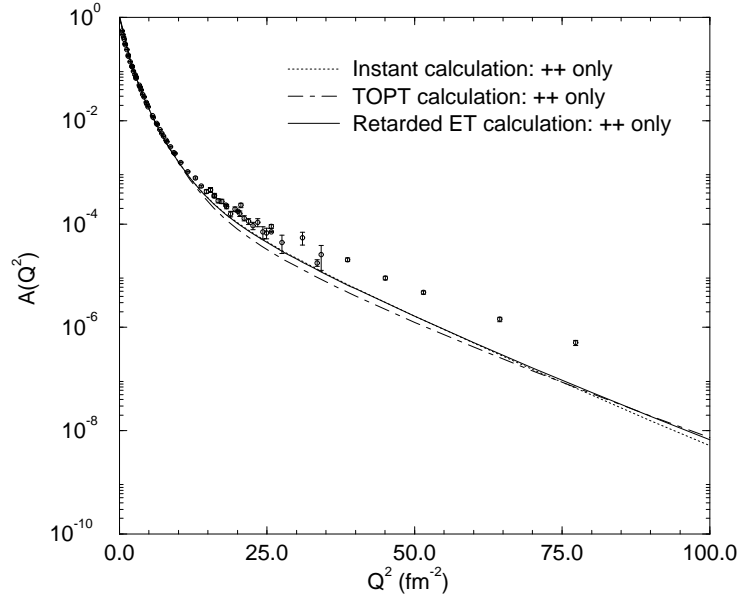


FIG. 6. The form factor  $A(Q^2)$  for the deuteron, as predicted by three different  $NN$  models. The dotted curve is the instant calculation, the dash-dotted curve is the calculation using the TOPT interaction, and the solid curve is the result using a retarded ET interaction. All calculations are done with the contributions of negative-energy states dropped.

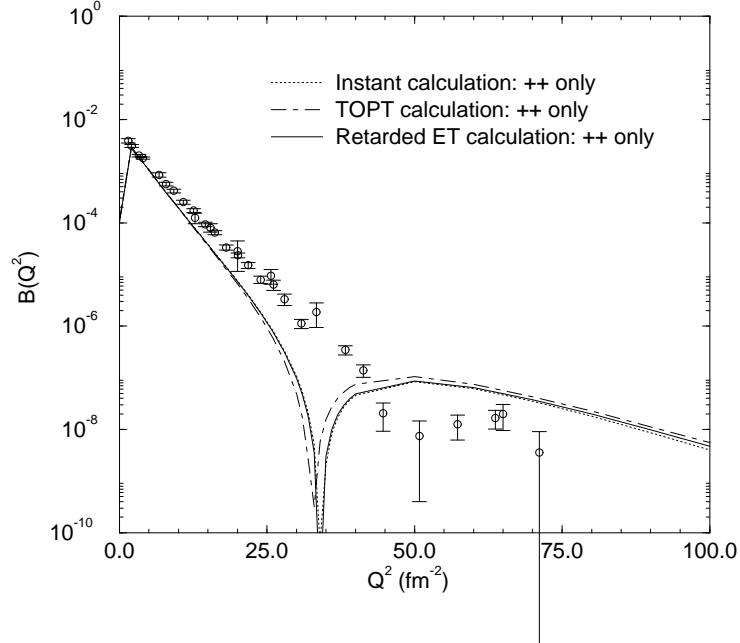


FIG. 7. The form factor  $B(Q^2)$  for the deuteron, legend as in Fig. 6. Again, all calculations are done in the  $++$  only approximation.

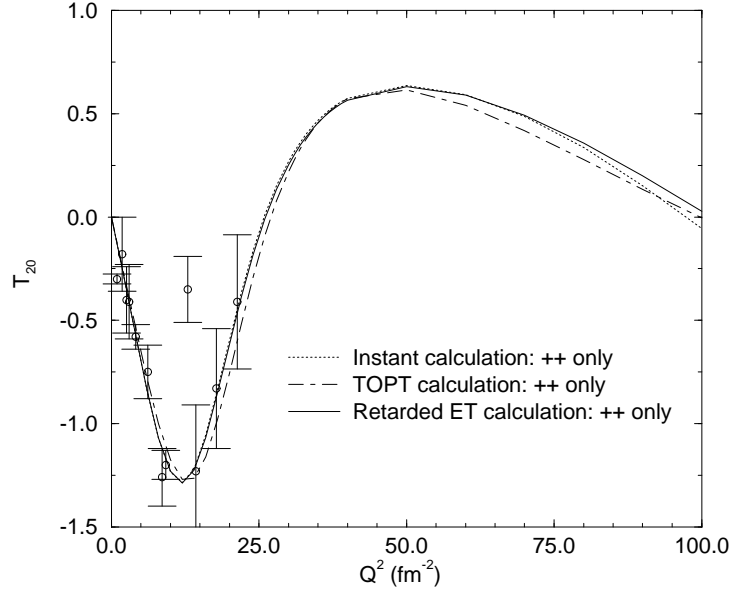


FIG. 8. The tensor polarization  $T_{20}(Q^2)$  in electron-deuteron scattering, legend as in Fig. 6. All calculations are done using only  $++$  states.

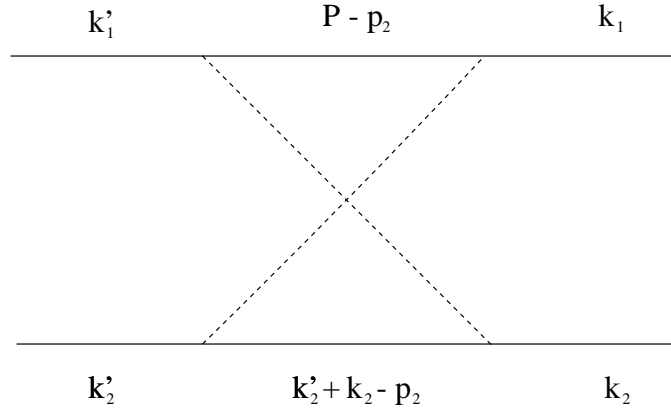


FIG. 9. The crossed-box graph, showing the momentum labels used in the text.



FIG. 10. The two time-ordered perturbation theory graphs for one-pion exchange.

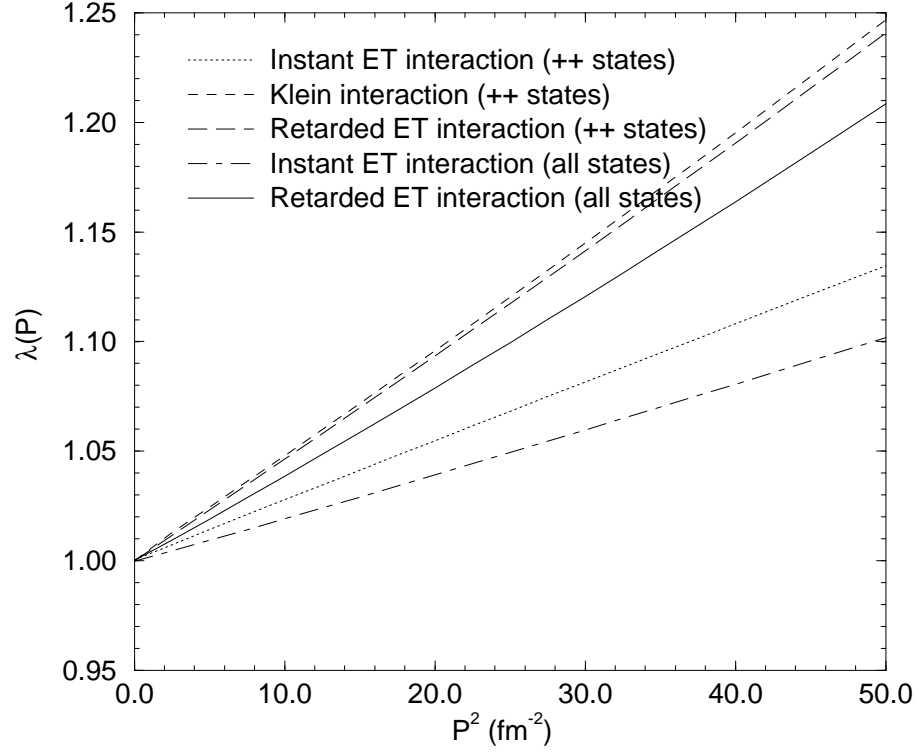


FIG. 11. A plot showing the eigenvalue,  $\lambda$ , of the homogeneous integral equation (2.26), as a function of the total three-momentum of the two-body system, for different choices of the interaction  $U_1$ . The dot-dashed (dotted) line is the result when  $U_1$  is chosen to be an instant interaction and all (only  $++$ ) states are included in the calculation. The solid (long dashed) line is the result when  $U_1$  is chosen to be the retarded interaction defined by Eq. (2.33) and all (only  $++$ ) states are included. Finally, the short-dashed line is the result from the TOPT interaction, calculated with  $++$  states only.



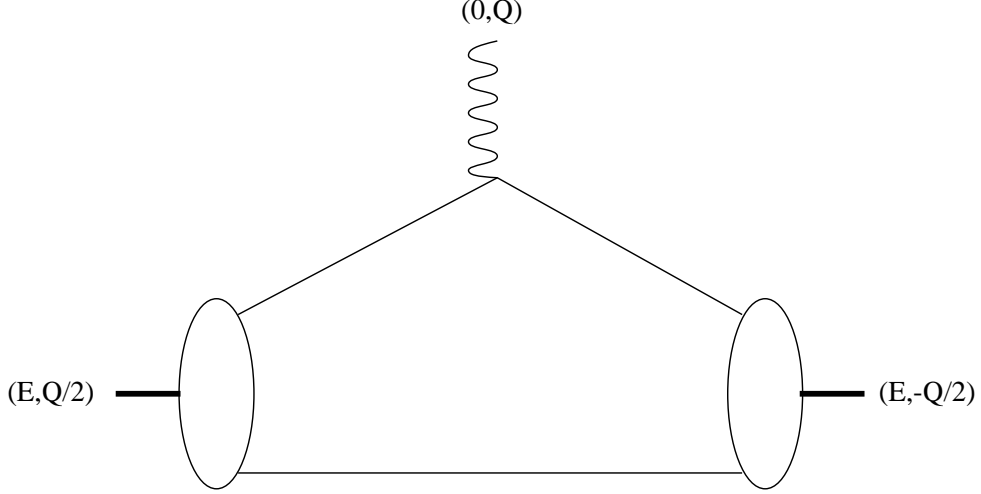


FIG. 12. The kinematics of electron-deuteron scattering, for a momentum transfer  $Q = (0, \mathbf{Q})$ , in the Breit frame.

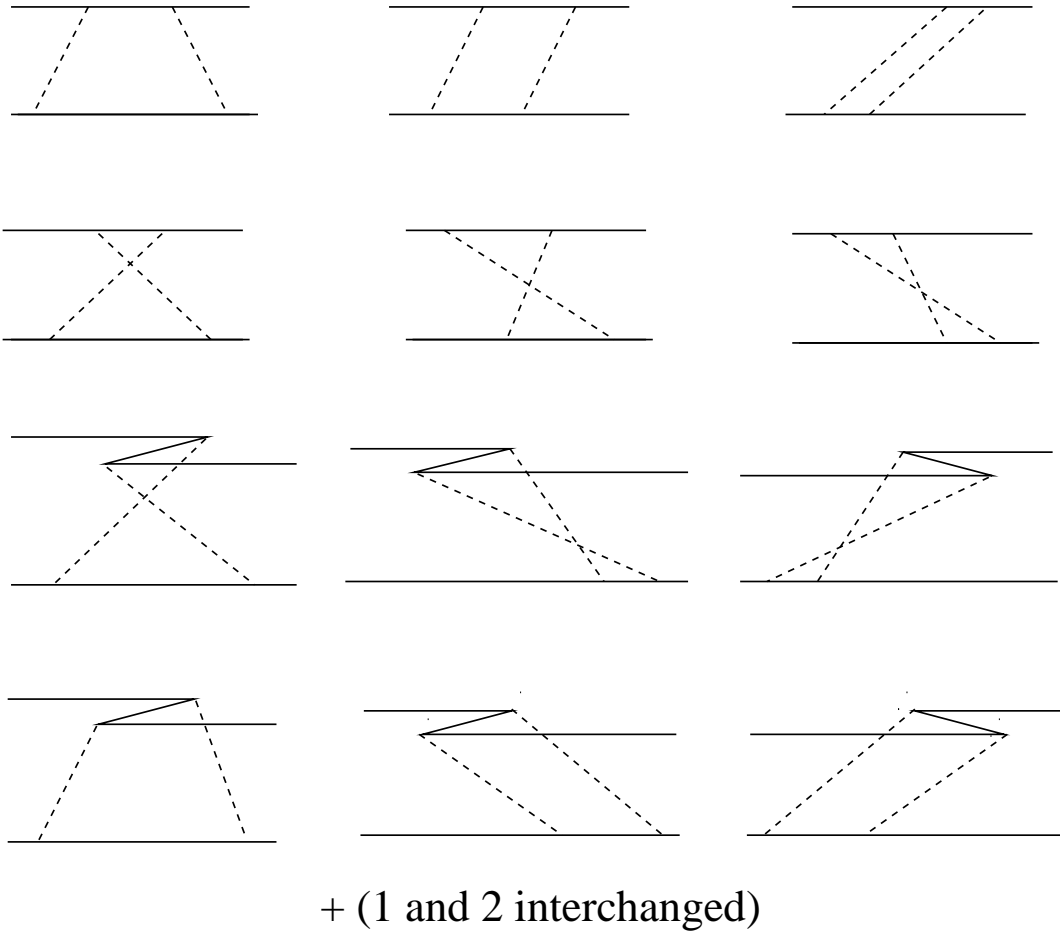


FIG. 13. The graphs which contribute to the three-dimensional  $NN$  t-matrix at fourth order in the coupling, up to order  $1/M$ . The graphs on the first and third line come from the  $NN$  Feynman box graph and those on the second and fourth line come from the  $NN$  Feynman crossed-box graph.

## REFERENCES

- [1] D. R. Phillips and S. J. Wallace, Phys. Rev. C **54**, 507 (1996), [nucl-th/9603008](#).
- [2] D. R. Phillips and S. J. Wallace, Few-body Systems (to appear), [nucl-th/9708027](#).
- [3] T. Nieuwenhuis and J. A. Tjon, Phys. Rev. Lett. **77**, 814 (1996).
- [4] E. E. Salpeter, Phys. Rev. **87**, 328 (1952).
- [5] A. Klein, Phys. Rev. **90**, 1101 (1953).
- [6] A. Klein, Phys. Rev. **94**, 1052 (1954).
- [7] A. A. Logunov and A. N. Tavkhelidze, Nuovo Cim. **29**, 380 (1963).
- [8] A. Klein and T.-S. H. Lee, Phys. Rev. D **10**, 4308 (1974).
- [9] A. D. Lahiff and I. R. Afnan, Phys. Rev. C **56**, 2387 (1997), [nucl-th/9708037](#).
- [10] V. B. Mandelzweig and S. J. Wallace, Phys. Lett. B. **197**, 469 (1987).
- [11] S. J. Wallace and V. B. Mandelzweig, Nucl. Phys. **A503**, 673 (1989).
- [12] F. Gross, Phys. Rev. **186**, 1448 (1969).
- [13] F. Gross, J. W. Van Orden and K. Holinde, Phys. Rev. **C45**, 2094 (1992).
- [14] R. Blankenbecler and R. Sugar, Phys. Rev. **142**, 1051 (1966).
- [15] E. Hummel and J. A. Tjon, Phys. Rev. Lett. **63**, 1788 (1989).
- [16] E. Hummel and J. A. Tjon, Phys. Rev. C **42**, 423 (1990).
- [17] E. Hummel and J. A. Tjon, Phys. Rev. C **49**, 21 (1994).
- [18] N. K. Devine and S. J. Wallace, Phys. Rev. C **48**, 973 (1993).
- [19] N. K. Devine and S. J. Wallace, Phys. Rev. C **51**, 3222 (1995).
- [20] J. E. Elias *et al.*, Phys. Rev. **177**, 2075 (1969).
- [21] R. G. Arnold *et al.*, Phys. Rev. Lett. **35**, 776 (1975).
- [22] G. G. Simon, C. Schmitt, and V. H. Walther, Nucl. Phys. **A364**, 285 (1981).
- [23] R. Cramer *et al.*, Z. Phys. C **29**, 513 (1985).
- [24] S. Platchkov *et al.*, Nucl. Phys. **A508**, 343 (1990).
- [25] S. Auffret *et al.*, Phys. Rev. Lett. **54**, 649 (1985).
- [26] P. Bosted *et al.*, Phys. Rev. C **42**, 38 (1990).
- [27] M. E. Schulze *et al.*, Phys. Rev. Lett. **52**, 597 (1984).
- [28] V. F. Dmitriev *et al.*, Phys. Lett. B. **157**, 143 (1985).
- [29] B. B. Voitsekhovskii *et al.*, JETP Lett. **43**, 733 (1986).
- [30] R. Gilman *et al.*, Phys. Rev. Lett. **65**, 1733 (1990).
- [31] I. The *et al.*, Phys. Rev. Lett. **67**, 173 (1991).
- [32] M. Ferro-Luzzi *et al.*, Phys. Rev. Lett. **77**, 2630 (1996).
- [33] J. W. van Orden, N. K. Devine, and F. Gross, Phys. Rev. Lett. **75**, 4369 (1995).
- [34] R. G. Arnold, C. E. Carlson, and F. Gross, Phys. Rev. C **21**, 1426 (1980).
- [35] M. J. Zuilhof and J. A. Tjon, Phys. Rev. C **24**, 736 (1981).
- [36] R. Machleidt, Adv. Nucl. Phys. **19**, 189 (1989).
- [37] J. L. Forest, V. R. Pandharipande, and J. L. Friar, Phys. Rev. C **52**, 568 (1995).
- [38] F. Gross and D. O. Riska, Phys. Rev. C **36**, 1928 (1987).
- [39] A. N. Kvinikhidze and B. Blankleider, Phys. Rev. C **56**, 2963 (1997), [nucl-th/9706051](#).
- [40] S. Mandelstam, Proc. Roy. Soc. (London) **233**, 248 (1955).
- [41] G. Hohler *et al.*, Nucl. Phys. **B114**, 505 (1976).